Research Square

Preprints are preliminary reports that have not undergone peer review.
They should not be considered conclusive, used to inform clinical practice,
or referenced by the media as validated information.

Multi-Omics Profiling of Female Ovary Development Identifies Key Defects in Seed Production of Autotetraploid Watermelon

Muhammad Zeeshan Sajjad
Henan Joint International Research Laboratory of South Asian Fruits and Cucurbits, Zhengzhou Fruit Research Institute, Chinese Academy of Agricultural Sciences

Xuqiang Lu
Henan Joint International Research Laboratory of South Asian Fruits and Cucurbits, Zhengzhou Fruit Research Institute, Chinese Academy of Agricultural Sciences

Eftekhar Mahmud
Henan Joint International Research Laboratory of South Asian Fruits and Cucurbits, Zhengzhou Fruit Research Institute, Chinese Academy of Agricultural Sciences

Fikru Tamiru Kenea
Henan Joint International Research Laboratory of South Asian Fruits and Cucurbits, Zhengzhou Fruit Research Institute, Chinese Academy of Agricultural Sciences

Mekonnen Tolasa Gonfa
Henan Joint International Research Laboratory of South Asian Fruits and Cucurbits, Zhengzhou Fruit Research Institute, Chinese Academy of Agricultural Sciences

Dongdong Yang
Henan Joint International Research Laboratory of South Asian Fruits and Cucurbits, Zhengzhou Fruit Research Institute, Chinese Academy of Agricultural Sciences

Gang Chen
Henan Joint International Research Laboratory of South Asian Fruits and Cucurbits, Zhengzhou Fruit Research Institute, Chinese Academy of Agricultural Sciences

Xiaowen Luo
Henan Joint International Research Laboratory of South Asian Fruits and Cucurbits, Zhengzhou Fruit Research Institute, Chinese Academy of Agricultural Sciences

He Nan
Henan Joint International Research Laboratory of South Asian Fruits and Cucurbits, Zhengzhou Fruit Research Institute, Chinese Academy of Agricultural Sciences

Hongju Zhu
Henan Joint International Research Laboratory of South Asian Fruits and Cucurbits, Zhengzhou Fruit Research Institute, Chinese Academy of Agricultural Sciences

Wenge Liu

liuwenge@caas.cn

Henan Joint International Research Laboratory of South Asian Fruits and Cucurbits, Zhengzhou Fruit Research Institute, Chinese Academy of Agricultural Sciences

---

Research Article

Keywords: Watermelon, seed number, Autotetraploidy, Pollen–pistil interaction, Ovule development, Transcriptome, Metabolome

Posted Date: July 15th, 2026

DOI: https://doi.org/10.21203/rs.3.rs-10078689/v1

License: This work is licensed under a Creative Commons Attribution 4.0 International License. Read Full License

Additional Declarations: No competing interests reported.

Title page

Full Title**:** Multi-Omics Profiling of Female Ovary Development Identifies Key Defects in Seed Production of Autotetraploid Watermelon

Authors:

Muhammad Zeeshan Sajjad[1], shan.sajjad@hotmail.com

Xuqiang Lu[1,2], luxuqiang@caas.cn

Eftekhar Mahmud, [1,3] eftekharmahmud@yahoo.com

Fikru Tamiru Kenea,[1,4] fikr1.kenea@gmail.com

Mekonnen Tolasa Gonfa, [1,5] mekonnen.tolasa@gmail.com

Yang Dongdong, [1,6] yddcaas@163.com

Chen Gang [1,7] cg147893@outlook.com

Luo Xiaowen, [1,2] luoxiaowen@caas.cn

Nan He [1,2] henan@caas.cn

Hongju Zhu [1,2]*, zhuhongju@caas.cn

Wenge Liu,[1]* liuwenge@caas.cn

[1.] Henan Joint International Research Laboratory of South Asian Fruits and Cucurbits, Zhengzhou Fruit Research Institute, Chinese Academy of Agricultural Sciences, Zhengzhou 450009, China.

[2]Zhongyuan Research Center, Chinese Academy of Agricultural Sciences, Xinxiang 453000, Henan, China.

[3] Bangladesh Agricultural Research Institute, Gazipur 1701, Bangladesh

[4] Department of Horticulture, College of Agriculture and Natural Resources, Dilla University, Ethiopia

[5] Ambo University, College of Agriculture and Veterinary Science, Department of Horticulture, Ambo, Ethiopia.

Contact information for corresponding authors:

Wenge Liu, (liuwenge@caas)

Hongju Zhu, (zhuhongju@caas.cn)

The Research Center of Fruit Preservation and Processing, Zhengzhou Fruit Research Institute, Chinese Academy of Agricultural Sciences, 450009, Zhengzhou, China.

Abstract

The autotetraploid watermelon lines serves as female parents to produce triploid seedless watermelon and their seed production directly impacts seed yield and high costing for triploid watermelon cultivars. Studying the key factors involved in autotetraploid seed production is critical for the triploid seedless watermelon programs. In this study, histological examination, antioxidant enzyme profiling, transcriptomic, and metabolomic analyses were employed to identify key developmental defects within the female ovary of the autotetraploid watermelon line K5M 4x which resulted in reduced seed production relative to the diploid line. Scanning electron microscopy revealed that diploid ovaries exhibited rapid pollen germination, directional pollen tube growth, and efficient penetration into the transmitting tract following pollination. In contrast, autotetraploid ovaries displayed delayed pollen germination, reduced pollen tube density, and aberrant tube morphology. Furthermore, ovary tissue analysis demonstrated that autotetraploid ovules were predominantly underdeveloped, resulting in significantly reduced seed set compared to the diploid line. Antioxidant enzyme activities including CAT, SOD, PPO, and POD were consistently elevated in autotetraploid ovaries, revealing enhanced oxidative stress and compensatory mechanisms. Transcriptomic analysis identified 1,027 and 686 differentially expressed genes at 1 DAP and 2 DAP, respectively, with enriched pathways including phenylpropanoid biosynthesis, plant hormone signal transduction, protein processing in the endoplasmic reticulum, and brassinosteroid biosynthesis. Metabolomic profiling revealed significant enrichment of tryptophan, tyrosine, starch and sucrose, and cysteine and methionine metabolic pathways. Integrated transcriptome–metabolome analysis revealed stage-specific gene–metabolite networks regulating auxin signaling, antioxidant enzyme homeostasis, and carbohydrate flux as primary determinants of impaired ovule development and reduced reproductive output in autotetraploid watermelon. These findings indicate that autotetraploidy alters pollen–pistil interactions and early ovule development, ultimately reducing reproductive efficiency in watermelon.

Key words Watermelon, seed number, Autotetraploidy, Pollen–pistil interaction, Ovule development, Transcriptome, Metabolome.

1. Introduction

Watermelon (Citrullus lanatus L.) is an important horticultural crop with the annual production of about 105 million metric tons worldwide with an area spanning over 3 million hectares (FAO 2024). It is cultivated worldwide for its economic impacts in agriculture as well as for its nutritional quality with rich water contents, higher lycopene and wide acceptability among its consumers (Tong et al., 2025**).** Watermelon is a monoecious species with separate male and female flowers on the same plant, fruit set is very much reliant on the appropriate formation, maturation and functionality of female floral organs (Sugiyama 2001). Triploid seedless watermelon is the predominant cultivation approach, representing 20% of watermelon production area in China and up to 80% in the United States, Southeast Asia, and South America (Wijesinghe et al., 2020).

Female flower fertility in watermelon is a complex trait that was governed by an intricate network of genetic, metabolic and hormonal interplay (Li et al., 2019). This process involves a series of developmental events that initiates with the establishment of floral meristem identity, followed by carpel differentiation and ovule initiation and pollen receptivity and post-pollination processes. These events were finely regulated by multilayered regulatory mechanisms acting at transcriptional, post-transcriptional and metabolic levels (Wang et al., 2021). Ethylene is known to be the key hormonal regulator for sexual expression in the cucurbitaceae family, with the effects not limited to sexual fate of individual floral buds but also impacts appearance of female flowers and number of female flowers per plant; (Martinez et al., 2021). Many hormones associated pathway with auxins, gibberellins (GAs), cytokinins (CKs), abscisic acid (ABA), and Jasmonates (JAs) also play their role in female floral growth, ovule development, and success in fertilization. Similarly, transcriptome and hormone profiling investigations in a variety of plant species revealed how different hormones crosstalk for early fruit set, where auxin and GA influence ovary growth and fruit initiation, cytokinin triggers cell division and ABA regulating seed development and dormancy (Baral et al., 2025).

Ovule production is an important developmental process in plant reproduction that involves the development of ovules as the precursors linked with female gametophyte (Gasser et al., 1998). The structural growth of ovules is an important aspect of number of seeds in a fruit, and it contributes to crop yield (Qadir et al., 2021). In angiosperms ovule growth is a complicated process that

involves complex mechanisms associated with gynoecium with multiple genes linked to ovule initiation and development of integument already been investigated in (*Arabidopsis thaliana)* (Duszynska et al., 2013). The key genes associated with brassinosteroid signaling genes involving *HLL, ANT,* and *AP2* that were associated with ovule production and development (Zumajo et al., 2020). Reactive oxygen species (ROS) function as indispensable signaling molecules that orchestrate ovule development and fertilization in fruit crops (Sankaranarayanan et al., 2020). The ovule development from initial morphogenesis to mature gametophyte formation is tightly linked with ROS dynamics (Cai et al., 2025). The balance between ROS production and scavenging act as key determinant for cell fate; excessive ROS can trigger programmed cell death (PCD), being necessary for specific developmental events like tapetal degradation in male gametophytes, must be strictly controlled in female tissues to prevent premature ovule senescence (Ye et al., 2021). Disruptions in this balance can lead to seed abortion, which in turn affects fruit size and shape, as observed in pummelo (*Citrus maxima*) where cross-pollination influences ovary development and fruit quality through physiological and transcriptomic adjustments (Wang et al., 2023)

Polyploidy being an important evolutionary event interlinked with various functional, morphological and genetic changes impacts fertility (Lloyd et al., 2016). RNA sequencing and metabolome profiling were used previously to identify the molecular mechanisms and problems associated with polyploidy for ovule development. The transcriptomic and metabolomic profiling for Chinese chestnut (*Castanea mollissima*), ovules revealed key regulatory pathways and metabolites associated with ovule abortion involving phytohormone signaling, energy metabolism, and amino acid pathways that were disrupted in polyploids (Cui et al., 2024) Similarly, transcriptome and metabolome for orchid (*Cymbidium sinense*), revealed starch and sucrose pathway followed by phenylpropanoid pathway and key enriched metabolites from secondary metabolite classes were involved for ovule development (Zeng et al., 2022). The transcriptome and metabolome studies of chickpea (*Cicer arietinum*) highlighted that MYB and bHLH transcription factors, C_2H_2 zinc finger proteins, ethylene responsive factors and WRKY gene family were also involved for ovule development (Singh et al.2023).

Triploid watermelon seed production requires crossing diploid male parents with autotetraploid female parents; the reciprocal cross consistently fails, yielding unfertilized empty seeds. Self-crossing of autotetraploid lines similarly results in markedly reduced seed set. Consequently,

autotetraploid seed production is a critical bottleneck in triploid breeding programs. Despite its agronomic importance, ovule development and its association with female fertility in autotetraploid watermelon remain unreported in the literature. To address this gap, we present the first comprehensive investigation integrating phenotypic characterization, antioxidant enzyme activity, transcriptomics (RNA-seq), and metabolomics to elucidate key pathways governing female flower fertility in autotetraploid watermelon.

2. Material and Methodology

2.1. Plant materials

The autotetraploid watermelon line (2n = 44) was developed from pure and homogenous diploid *C. lanatus* isogenic line K5M (2n = 22). Polyploidy was induced as described by (Zhou et al., 2018). The seeds were pretreated and germinated in a growth chamber, nurseries were planted in greenhouses, and field planation of the seedlings was carried out for two spring seasons. The seeds of the mature fruits were counted at harvest where diploid watermelon line k5M 2x produced more seeds than the autotetraploid watermelon line K5M 4x.

2.2. Observation of pollen tube germination in the female flower

The female flowering buds were selected from every second and third node after 1 day after pollination (1 DAP) and 2 day after pollination (2 DAP) and were preserved in 4% glutaraldehyde and stored in dark at 4 °C overnight. Later, these samples were washed with phosphate buffer and immersed in 1% osmium tetra oxide for 1-2 hours and rinsed with the phosphate buffer. Afterwards these ovaries were dipped in different series of ethanol for 15 minutes to achieve required dehydration. The critical freeze drying was obtained by using carbon dioxide. The tissues were kept on the aluminum stub and coated with gold particles for 90 seconds and stigma portion was focused on obtaining high resolution images at different magnification ranges using HITACHI Regulus 8100 scanning electron microscope.

2.3. Paraffin sectioning of female flower to observe ovule development

To perform the histological analysis of the female ovary, samples were harvested for 1 day after pollination (1 DAP) and 2 day after pollination (2 DAP) from every second and third node of plant and were subsequently fixed in FAA solution. Later, these samples were dissected using the stereo

microscope and horizontal sections were cut and fixed in paraffin blocks. After fixation these blocks were sliced in to thin sections using microtome and slices for 7–10 µm were cut and dehydrated in a series of ethanol for 2 hours and samples were cleared by using xylene and these samples were mounted on the slides and stained with toluidine blue dye and tissues were further rinsed with water for 2 minutes and oven dried and Nikon Eclipse E 100 and Nikon DS- U3 imaging system were used to take the images.

2.4. Measurement of antioxidant activities for ovary tissues at different pollination intervals

The female flower ovaries were collected at one day after pollination and two days after pollination and flower samples were preserved in liquid nitrogen and samples were preserved in cryogenic refrigerator at -80 °C. The Qiagen tissue homogenizer was utilized to grind and homogenize the samples into powder form. After grinding 1 gram of powder sample was dissolved in 4 ml phosphate buffer and were centrifuged for 15 minutes at 10000 rpm at 4 °C. In order to measure the peroxidase (POD) 200 ul of sodium phosphate buffer was mixed with guanicol, H_2O_2, and enzyme supernatant and the absorbance was recorded at short time intervals at 465nm wavelength of light (Nabi et al., 2020) For measuring the polyphenol oxidase (PPO) the 100 ul of sodium phosphate buffer was added with 50 ul of catechol and 50ul of tissue supernatant was used and readings were taken four to five times in the intervals of 2 to 5 minutes at 405 nm (Kiani et al., 2021).. To calculate the super oxidase dismutase (SOD) measuring kit (G4306 Beijing Solarbio Science & Technology CO., LTD Beijing, China) was provided followed by (G4307 Beijing Solarbio Science & Technology CO., LTD Beijing, China) that was used to measure catalase enzyme (CAT).

2.5. RNA extraction and library preparation

The female flowers of diploid and autotetraploid watermelon line were selected after 1DAP and 2 DAP and these samples were classified into two groups. The 1 DAP samples were designated as E_Vs_F, and the samples of 2 DAP were named G_Vs_H. Total RNA was extracted by trizol method with modifications by adding 1% marceptoethanol as per manufacturer protocol (Thermo Fisher Scientific Inc. USA). The quantity of the RNA was evaluated with the Nanodrop spectrophotometer. 1µg total RNA was used for following library preparation using RNA Sample Prep Kit (Illumina, USA). The libraires were than sequenced with Illumina HiSeq™ 2000 system. The watermelon reference genome V2 (97102) was used from the Cucurbits Genomics Database

for alignment. The clean reads for watermelon using the V2 genome were obtained using Bowtie 2 and Top HAT 2 (Langmead et al., 2012; Kim et al., 2013). The functional annotation analysis of differentially expressed genes (DEGs), gene ontology (GO), KEGG pathway and gene description was determined by using egg NOG online software (http://eggnog-mapper.embl.de/). R software was used to draw the volcanic plot, gene expression heatmap, and KEGG enrichment.

2.6. qRT-PCR for verification of DEGs in RNA seq data

Quantitative real-time PCR (qRT-PCR) was used to analyze and verify the DEGs analyzed by RNA seq. RNA extraction from the diploid and autotetraploid female flower samples at1DAP and 2DAP was carried out by FLA Pure RNA extraction kit by TOLO BIO Science. cDNA was synthesized from RNA by using Tolo Script All in one RT Easymix from total RNA. qRT- PCR was performed for by using 2*Q3 SYBR qPCR Master Mix (Universal) for qPCR by TOLOBIO using ROCHE Light Cycler 480 by ROCHE Switzerland. The gene sequences were taken from watermelon genome database reference genome V2. After designing online primers watermelon *ClACT* was used as control, and gene expressions were quantified by using $2^{-\Delta\Delta Ct}$ method (Livak and Schmittgen 2001). Primers were given in table S1.

2.7. Un targeted metabolome analysis for female flower samples.

Female flower buds were collected from the diploid and autotetraploid watermelon line and the samples were prepared and untargeted metabolites in ovary samples were identified by using UPLC-Q-TOF/MS system. The UPLC and MS conditions were similar as reported by (Nawaz et al., 2026). R software (www.r-project.org) was used to perform multivariate analysis. Identified metabolites were annotated using Kyoto Encyclopedia of Genes and Genomes database (http://www.kegg.jp/kegg/compound/) and annotated metabolites were then mapped to KEGG (http://www.kegg.jp/kegg/pathway.html) pathways.

2.8. Data analysis.

All experiments were conducted with biological replicates, and data are presented as mean ± standard error (SE). Differences in seed number, ovule counts, developmental percentages, and antioxidant enzyme activities (CAT, SOD, POD, PPO) between diploid (K5M 2x) and autotetraploid (K5M 4x) lines at 1 and 2 days after pollination (DAP) were assessed using a T test and one-way analysis of variance (ANOVA) by GraphPad prism 10.1.2 and graphs were drawn.

Statistically distinct groups were indicated by different letters above bars in the figures with a significance threshold of $P < 0.05$. TB tools was used to draw the heatmaps showing variation for gene expressions and Origin pro 2020 was used to draw the correlation for gene and metabolite expression.

3. Results

3.1. Pollen Tube germination in diploid and autotetraploid watermelon ovaries.

Scanning electron microscopy (SEM) of K5M 2x ovaries showed that at 4 hours after pollination (HAP), numerous pollen grains were firmly attached to the stigmatic surface. Many of these had already begun to germinate, with visible pores from which pollen tubes were emerging. At this stage, however, the tubes were relatively few and largely restricted to the stigma, and only limited penetration into the stigmatic tissues was observed (Fig. 1A, B). By 8 HAP, both pollen tube density and elongation had increased noticeably. The stigmatic surface appeared densely colonized, and many tubes had entered the underlying tissues, progressing toward the transmitting tract. The growth pattern was clearly directional, suggesting effective guidance by the female reproductive tissues (Fig. 1C, D). At 12 HAP, extensive pollen tube growth was evident within the stylar region. Numerous elongated tubes were present in the transmitting tract, indicating continued progression through the style. The stigma and style remained structurally intact and receptive to pollen tube growth (Fig. 1E, F).

In contrast, K5M 4x female ovaries at 4 HAP showed pollen grains present on the stigmatic surface but with relatively low germination. The few germinating grains produced short, irregular tubes, and penetration into the stigmatic tissue was minimal, indicating a delayed onset of growth (Fig. 1G, H). At 8 HAP, although the number of germinating pollen grains increased, tube elongation remained limited. Many tubes displayed abnormal features such as swelling and irregular growth paths. Penetration into the transmitting tissues was inconsistent, and a substantial number of ungerminated or partially germinated grains remained on the stigma, pointing to reduced efficiency and disrupted pollen tube development (Fig. 1I, J). By 12 HAP, only a small number of thin pollen tubes were observed in the stylar region, and their distribution was sparse and discontinuous. Signs of growth arrest, including enlarged tube tips, were evident, and colonization of the transmitting tract remained limited (Fig. 1K, L). Overall, tetraploid female ovaries showed delayed germination, reduced pollen tube elongation, and structural abnormalities across developmental stages. These

patterns suggest impaired pollen–pistil interactions and reduced efficiency of pollen tube progression toward the ovary.

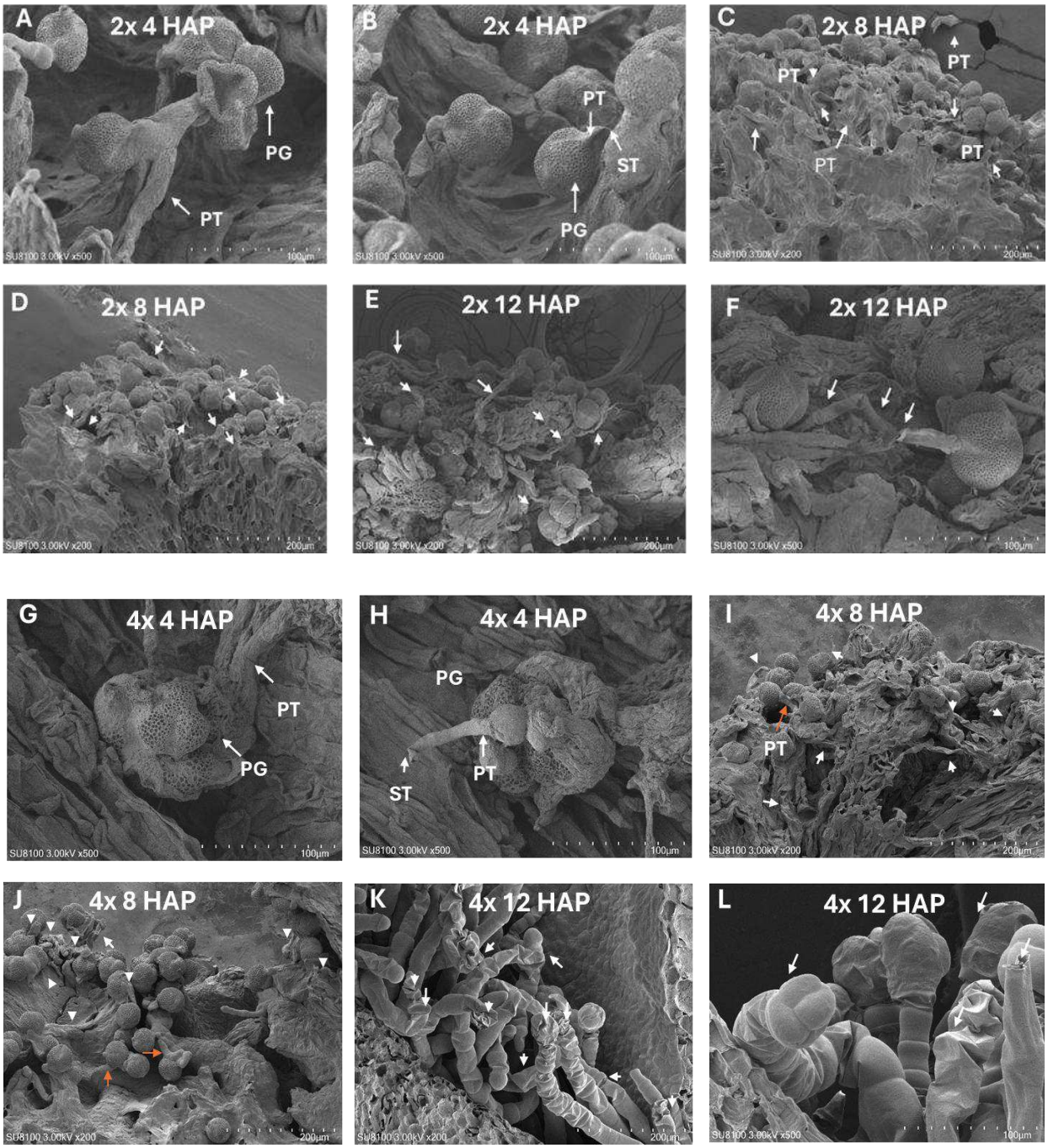


Figure 1. The SEM observation of pollen germination and pollen tube growth in different time intervals in diploid watermelon line K5M 2x and autotetraploid watermelon line K5M 4x. (A) At 4h after pollination the pollen tubes have emerged from the germinal aperture. (B) At

4h after pollination the pollen tubes had initiated to penetrate the stigma. (C) At 8h after pollination maximum pollen tubes have germinated. (D) At 8h after pollination maximum pollen tubes have penetrated the stigma. (E) At 12h after pollination maximum number of pollen tubes have been germinated. (F) At 12h after pollination a pollen tube increased its length and encircling the stigma (G) At 4 h after pollination the pollen tubes have emerged from the germinal aperture. (H) At 4h after pollination pollen tubes had initiated to penetrate the stigma (I) At 8 h after pollination maximum pollen tubes have failed to germinate except one. (J) At 8 h after pollination maximum pollen tubes have failed to penetrate the stigma except two. (K) At 12 h after pollination maximum number of pollen tubes have abnormal germination and pollen tubes are ruptured or folded. (L) At 12 h after pollination the pollen tubes heads are swollen and ruptured and failed to penetrate stigma.

3.2. Ovules and seed development in diploid and autotetraploid watermelon female ovary after 1DAP and 2 DAP.

Histological and quantitative analyses revealed clear ploidy-dependent variation in ovule development and reproductive output. Transverse sections of diploid K5M 2x ovaries showed a higher number of well-developed ovules compared with autotetraploid K5M 4x ovaries at both 1 and 2 days after pollination (DAP). At 1 DAP, most ovules in diploid K5M 2x ovaries were well organized and exhibited steady growth. In contrast, ovules in autotetraploid K5M 4x ovaries were often disorganized and showed abnormal development (Fig.2A, B). These anatomical observations were consistent with the quantitative analysis. At 2 DAP, the number of ovules increased significantly compared with 1 DAP in both ploidy levels; however, ovule number remained consistently higher in diploid ovaries than in tetraploid ovaries. Similarly, the proportion of developed ovules was markedly higher in diploid ovaries (Fig.2C). At 1 DAP, half of the ovules in diploid ovaries reached advanced developmental stages, half ovaries exhibited a lower proportion of developed ovules. By 2 DAP, ovule development improved in both ploidy levels; however, the difference between them persisted, with diploids showing twofold higher developmental efficiency than tetraploids (Fig.2D). Overall, diploid ovaries exhibited superior ovule development and higher developmental efficiency compared with tetraploid ovaries.

The reduced ovule numbers and decreased developmental efficiency in autotetraploid K5M 4x ovaries had reduced the reproductive performance. Seed set analysis depicted a substantial decline in total seed number in autotetraploid watermelon line K5M 4x compared with diploid watermelon

line K5M 2x. The visual comparison further verified that the successful development of normal seeds is lower in tetraploids, whereas diploids produced abundant and uniformly developed seeds (Fig.2E, F). Collectively, these results suggest that autotetraploidy impacted early ovule development, leading to reduced ovule fertility and decreased seed set. The continuity of underdeveloped ovules during the early post-pollination period suggests that impaired ovules represent a primary cause of reduced reproductive efficiency in autotetraploid watermelon lines.

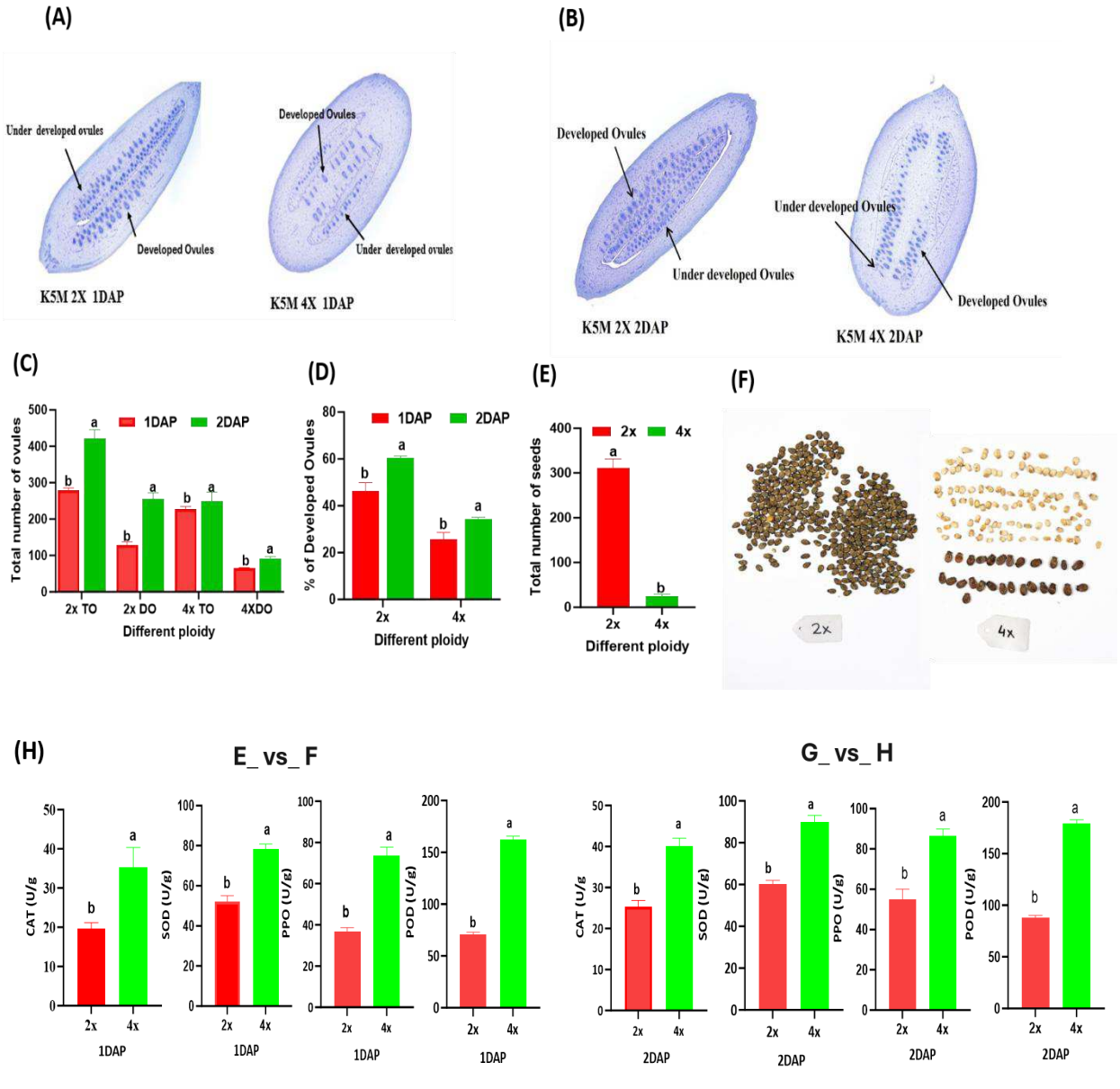


Figure 2. Comparative analysis of ovule development, seed formation, and antioxidant enzyme activities in diploid (2x) and autotetraploid (4x) watermelon line K5M. (A) Longitudinal sections of ovaries at 1 day after pollination (1DAP) showing the distribution of developed and underdeveloped ovules in K5M 2x and K5M 4x plants. The diploid ovary displays a higher proportion of normally developed ovules compared with the autotetraploid line. (B) Ovary sections at 2 days after pollination (2DAP) illustrating ovule development patterns in diploid and autotetraploid plants. The diploid genotype exhibits a greater number of developed ovules, whereas the tetraploid line shows a higher frequency of underdeveloped ovules. (C) Quantification of the total number of ovules in different ploidy combinations at 1DAP and 2DAP, including 2xTO, 2xDO, 4xTO, and 4xDO. (D) Percentage of developed ovules in diploid and autotetraploid plants at 1DAP and 2DAP, indicating reduced ovules in the tetraploid line. (E) Total number of seeds per fruit harvested in Spring 2024, showing significantly higher seed production in diploid plants compared with autotetraploid plants. (F) Representative images of mature seeds collected from diploid (2x) and autotetraploid (4x) fruits. (G) Activities of antioxidant enzymes including catalase (CAT), superoxide dismutase (SOD), and peroxidase (POD) in ovaries of diploid and autotetraploid plants at 1DAP and 2DAP. Enzyme activities were generally higher in the autotetraploid plants compared with the diploid counterparts. Bars represent mean ± standard error, and different letters above the bars indicate statistically significant differences between treatments ($P < 0.05$)

3.3. Antioxidant enzyme activity in diploid and autotetraploid watermelon ovaries across different pollination intervals

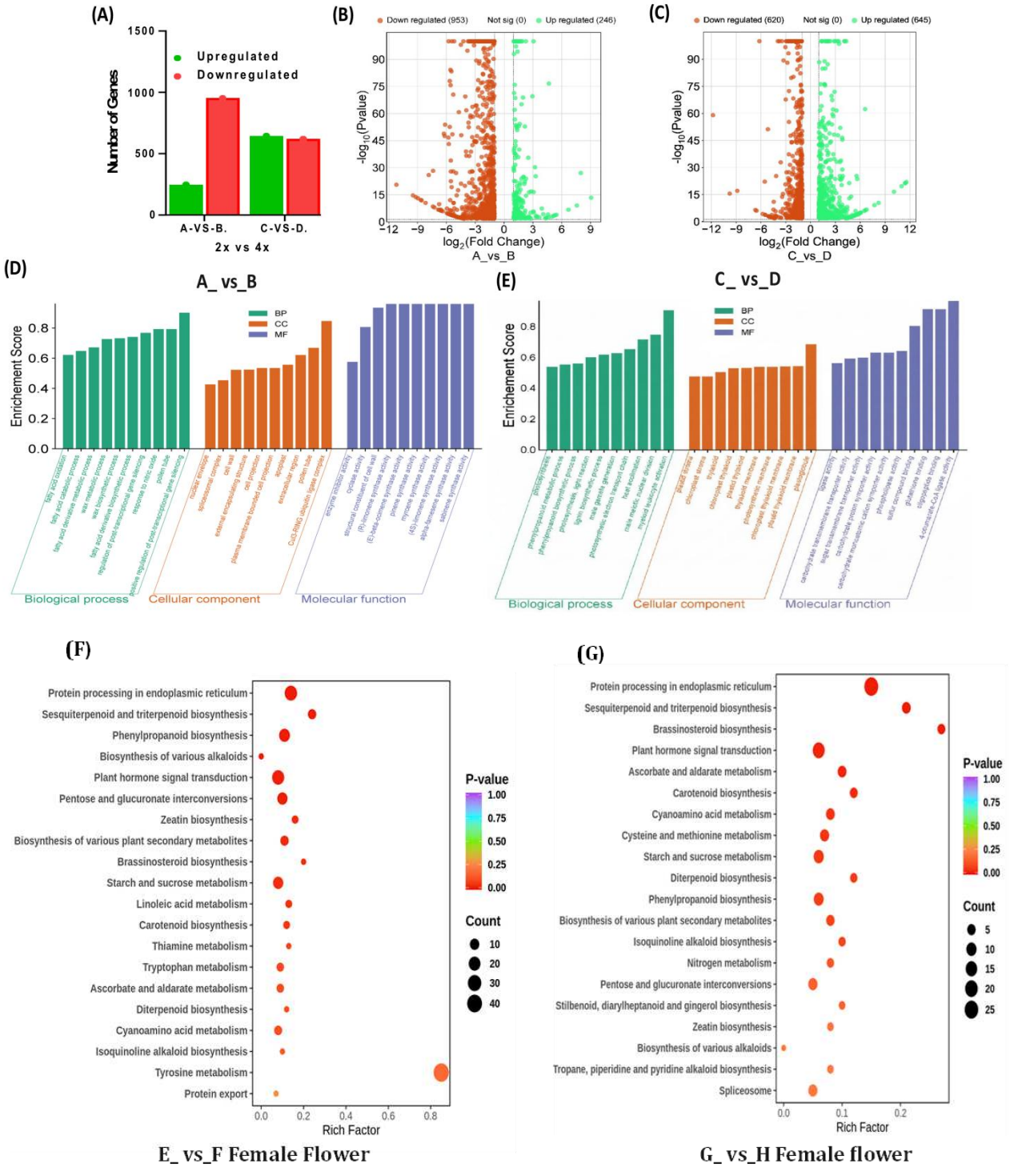
Antioxidant enzyme activities were measured in diploid K5M 2x and autotetraploid K5M 4x ovary tissues at 1 and 2 days after pollination (DAP) to observe their oxidative status during early developmental stages after pollination. After 1 DAP, autotetraploid ovary tissues displayed increased activities of CAT, SOD, PPO, and POD relative to 2x exhibited markedly higher activities of CAT, SOD, PPO, and POD relative to 2x, with increases of approximately 75 to 130% depending on the enzyme. CAT activity increased from 20 to 35 U/g, SOD from 50 to 80 U/g, PPO from 35 to 75 U/g, and POD from 70 to 165 U/g. A similar trend was observed on 2 DAP with the autotetraploid having significantly higher activities of CAT, SOD, PPO and POD CAT increased from 25 to 40 U/g, SOD from 60 to 90 U/g, PPO from 55 to 85 U/g, and POD from 90 to 180 U/g respectively (Fig.2H). Overall, systematic elevation of antioxidant enzyme activities between autotetraploid ovary tissues devises more efficient ROS-scavenging system than diploids. This improved antioxidative capacity might be associated with maintenance of cellular redox homeostasis, protection of reproductive tissues against oxidative damages, and processes in the early post-pollinated stage.

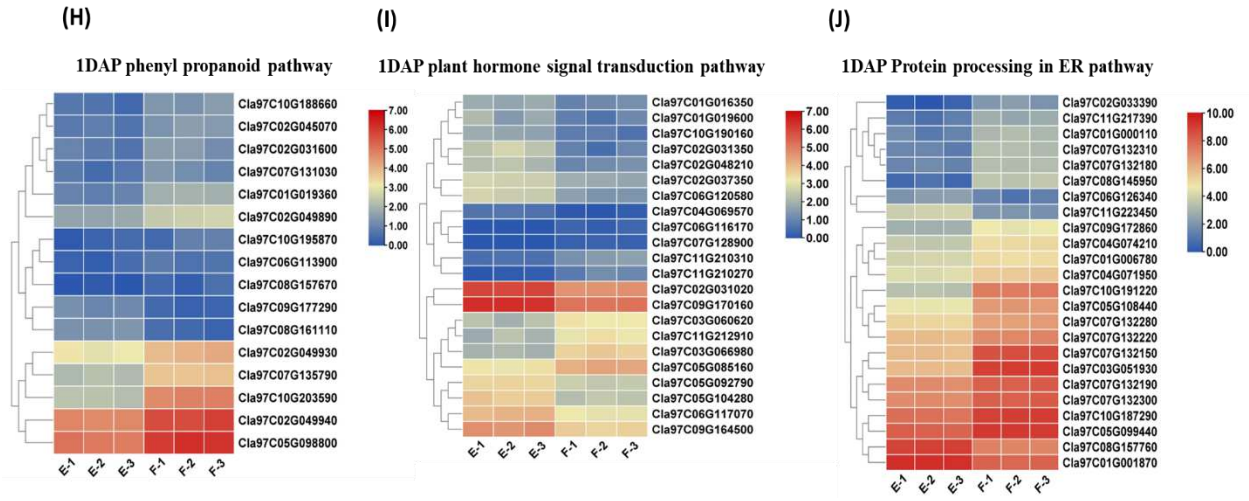
3.4. Transcriptome profiling and functional enrichment analysis of diploid and autotetraploid watermelon ovaries

The female flowers at 1 and 2 days after pollination were sampled from diploid K5M 2x and autotetraploid K5 M 4x for transcriptome indicated as E_vs_F (1 DAP) and G_vs_H (2 DAP). After quality filtering 468,576,064 clean reads were generated with Q20 values ranging from 97.53 to 98.59% and Q30 values around 95%, quality of results favor subsequent analysis that involved the alignment with the reference genome 97,103 (V2). The bar graphs reveal the total number of differentially expressed genes for all the experimental groups (Fig.3A). E_Vs _F comparison showed that 1,027 differentially expressed genes (DEGs) were identified, 472 genes were upregulated, and 555 were downregulated (Fig.3B) and table S2. Likewise, G_Vs_H comparison provided 686 DEGs with 215 up- and 471 down-regulated genes (Fig.3C) and table S3. The gene ontology enrichment analysis enrichment score ranged from 0.0 to 0.8 and DEGs were enriched for top 30 different enriched Go terms for all samples. (Fig. 3D, E). The enriched biological process (BP) categories in the E_Vs_F dataset were mostly linked to nucleic acid metabolism, DNA replication and transcription regulation, RNA processing, and cell cycle-related processes. Terms involved in cellular components (CC) were highly enriched with nucleus, chromatin, chromosome, and other structures of the cell while the molecular functions (MF) terms were nucleic acid binding, transcription factor activity, ATP binding and protein kinase activity.

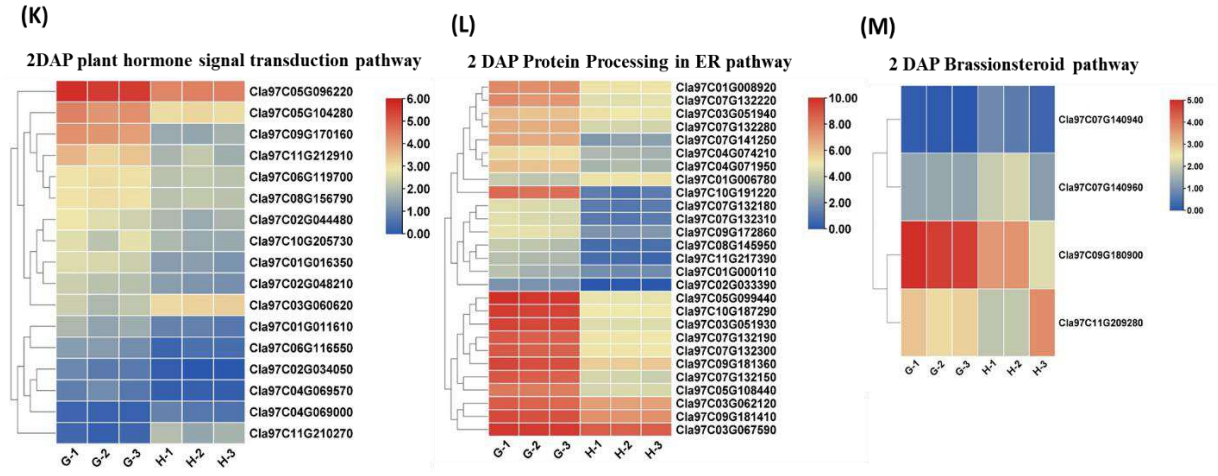
These results indicate active regulation of cell division, gene expression, and chromatin dynamics during early developmental transitions. (Fig. 3D). Enriched BP terms in the G_VS_H comparison related to the responses to endogenous stimuli, hormone-mediated signaling, stress responses, metabolic processes, and cellular organization. CC enrichment was composed of cytoplasm, plasma membrane and organelle-associated substances. The catalytic activity, oxidoreductase activity, transferase activity and other binding functions dominated the MF categories (Fig. 3E). The KEGG pathway analysis revealed key metabolic and regulatory functions associated with female flower development at 1DAP and 2DAP.The highly enriched pathways for 1DAP involved protein processing in endoplasmic reticulum, sesquiterpenoids and triterpenoid pathway, phenylpropanoid biosynthesis, biosynthesis of various alkaloids and plant hormone signal transduction (Fig. 3F). Similarly top five the highly enriched pathways for 2 DAP female flower development were protein processing in endoplasmic reticulum, sesquiterpenoids and triterpenoid

pathway, plant hormone signal transduction, brassionsteroid biosynthesis pathway and ascorbate and Alderete metabolism pathway (Fig. 3G).




(H)
1DAP phenyl propanoid pathway
Cla97C10G188660
Cla97C02G045070
Cla97C02G031600
Cla97C07G131030
Cla97C01G019360
Cla97C02G049890
Cla97C10G195870
Cla97C06G113900
Cla97C08G157670
Cla97C09G177290
Cla97C08G161110
Cla97C02G049930
Cla97C07G135790
Cla97C10G203590
Cla97C02G049940
Cla97C05G098800
E-1 E-2 E-3 F-1 F-2 F-3
7.00 6.00 5.00 4.00 3.00 2.00 1.00 0.00
(I)
1DAP plant hormone signal transduction pathway
Cla97C01G016350
Cla97C01G019600
Cla97C10G190160
Cla97C02G031350
Cla97C02G048210
Cla97C02G037350
Cla97C06G120580
Cla97C04G069570
Cla97C06G116170
Cla97C07G128900
Cla97C11G210310
Cla97C11G210270
Cla97C02G031020
Cla97C09G170160
Cla97C03G060620
Cla97C11G212910
Cla97C03G066980
Cla97C05G085160
Cla97C05G092790
Cla97C05G104280
Cla97C06G117070
Cla97C09G164500
E-1 E-2 E-3 F-1 F-2 F-3
7.00 6.00 5.00 4.00 3.00 2.00 1.00 0.00
(J)
1DAP Protein processing in ER pathway
Cla97C02G033390
Cla97C11G217390
Cla97C01G000110
Cla97C07G132310
Cla97C07G132180
Cla97C08G145950
Cla97C06G126340
Cla97C11G223450
Cla97C09G172860
Cla97C04G074210
Cla97C01G006780
Cla97C04G071950
Cla97C10G191220
Cla97C05G108440
Cla97C07G132280
Cla97C07G132220
Cla97C07G132150
Cla97C03G051930
Cla97C07G132190
Cla97C07G132300
Cla97C10G187290
Cla97C05G099440
Cla97C08G157760
Cla97C01G001870
E-1 E-2 E-3 F-1 F-2 F-3
10.00 8.00 6.00 4.00 2.00 0.00

349


(K)
2DAP plant hormone signal transduction pathway
Cla97C05G096220
Cla97C05G104280
Cla97C09G170160
Cla97C11G212910
Cla97C06G119700
Cla97C08G156790
Cla97C02G044480
Cla97C10G205730
Cla97C01G016350
Cla97C02G048210
Cla97C03G060620
Cla97C01G011610
Cla97C06G116550
Cla97C02G034050
Cla97C04G069570
Cla97C04G069000
Cla97C11G210270
G-1 G-2 G-3 H-1 H-2 H-3
6.00 5.00 4.00 3.00 2.00 1.00 0.00
(L)
2 DAP Protein Processing in ER pathway
Cla97C01G008920
Cla97C07G132220
Cla97C03G051940
Cla97C07G132280
Cla97C07G141250
Cla97C04G074210
Cla97C04G071950
Cla97C01G006780
Cla97C10G191220
Cla97C07G132180
Cla97C07G132310
Cla97C09G172860
Cla97C08G145950
Cla97C11G217390
Cla97C01G000110
Cla97C02G033390
Cla97C05G099440
Cla97C10G187290
Cla97C03G051930
Cla97C07G132190
Cla97C07G132300
Cla97C09G181360
Cla97C07G132150
Cla97C05G108440
Cla97C03G062120
Cla97C09G181410
Cla97C03G067590
G-1 G-2 G-3 H-1 H-2 H-3
10.00 8.00 6.00 4.00 2.00 0.00
(M)
2 DAP Brassionsteroid pathway
Cla97C07G140940
Cla97C07G140960
Cla97C09G180900
Cla97C11G209280
G-1 G-2 G-3 H-1 H-2 H-3
5.00 4.00 3.00 2.00 1.00 0.00

350

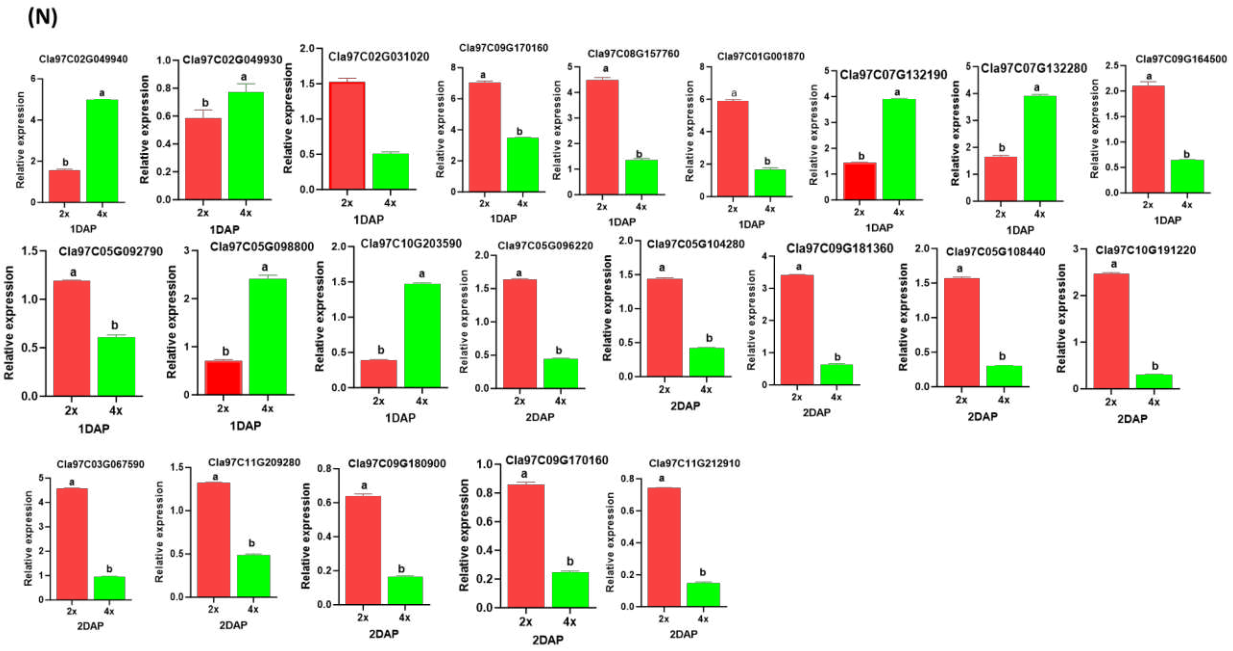


Figure 3. **Transcriptome analysis and pathway enrichment and qPCR expression of Differential Expressed Genes (DEGs) in female flowers at 1DAP and 2DAP**. (A) Number of upregulated and downregulated genes identified in comparisons E_vs_F (1DAP) and G_vs_H (2DAP). (B) and G_vs_H (C). Red dots represent significantly upregulated genes; green dots represent significantly downregulated genes. D–E) Gene Ontology (GO) enrichment analysis for E_vs_F (D) and G_vs_H (E), categorized into biological process, cellular component, and molecular function. (F–G) KEGG pathway enrichment dot plots for E_vs_F (F, 1DAP) and G_vs_H (G, 2DAP). Dot size indicates gene count, and color scale reflects adjusted p-value. (H–J) Heatmaps of representative pathways in 1DAP female flowers: phenylpropanoid biosynthesis (H), plant hormone signal transduction (I), and protein processing in the endoplasmic reticulum (J). (K–M) Heatmaps of representative pathways in 2DAP female flowers: plant hormone signal transduction (K), protein processing in the endoplasmic reticulum (L), and brassinosteroid biosynthesis (M). (N) Quantitative RT-PCR validation of selected differentially expressed genes identified from transcriptome analysis. Each bar represents the mean relative expression level (± standard error) under diploid (2x) and tetraploid (4x) conditions at 1DAP or 2DAP. Statistical significance between ploidy levels is indicated by different letters above the bars ($P < 0.05$).

3.5. KEGG pathways enriched for diploid and autotetraploid female ovary development at 1 DAP and 2 DAP.

3.6. Phenyl propanoid pathway

The phenylpropanoid pathway involved around sixteen genes, among which fourteen were upregulated while two genes were downregulated (Fig. 3H). The upregulated genes involved *Cla97C10G188660* producing Caffeic acid 3-O-methyltransferase, *Cla97C10G195870* linked

with cinnamoyl reductase and *Cla97C02G031600* that synthesized cytochrome P450 84A1-like enzymes. The peroxidase gene family upregulated genes involved *Cla97C01G019360, Cla97C02G045070, Cla97C02G049930, Cla97C05G098800, Cla97C06G113900, Cla97C07 G1--31030, Cla97C07G135790* were upregulated while *Cla97C09G177290* was suppressed. Similarly, the *Cla97C02G049890, Cla97C02G049940, Cla97C10G203590, Cla97C08G157670* were the members of peroxidase gene family involved in the removal of H_2O_2 hydrogen per oxide, biosynthesis and degradation of lignin and oxidative stress caused by environmental stimuli while *Cla97C08G161110* linked to vinorine synthase was suppressed.

3.7. Plant hormone signal transduction pathway.

In the plant hormone signal transduction pathway, there were twenty-two genes involved among which fourteen genes were downregulated, and seven genes were upregulated for autotetraploid watermelon line K5M 4x female flowers at 1DAP (Fig. 3I). Auxin-related gene families constituted the predominant component of this pathway. The auxin transporter family had *Cla97C11G210270* with elevated expression whereas the other two genes *Cla97C04G069570,* Cla97C01G016350 were repressed. The GH3 protein family involved *Cla97C05G092790* that was downregulated while *Cla97C05G092790, Cla97C11G212910* were upregulated. All the genes from auxin responsive proteins were *Cla97C02G031020, Cla97C02G031350, Cla97C02G037350 Cla97C02G048210, Cla97C06G120580, Cla97C09G170160* were suppressed while one gene *Cla97C05G085160* expression was elevated. Auxin-responsive protein SAUR21-like gene family with *Cla97C05G104280, Cla97C09G164500, Cla97C11G210310* were also downregulated. Similarly, genes *Cla97C11G210310* from auxin-responsive protein SAUR50, followed by *Cla97C03G066980* ERF 1B and *Cla97C03G060620* from protein kinase was upregulated. While Cla97C01G019600 bZIP transcription factor, *Cla97C06G117070* abscisic acid receptor and another *Cla97C10G190160* histidine encoding phosphotransfer protein and were also suppressed.

For the female flower 2 DAP in the autotetraploid watermelon line K5M 4x there were seventeen genes involved among which fourteen were downregulated and three genes were up regulated (Fig. 3K). The significantly upregulated genes involved *Cla97C03G060620* auxin transporter-like protein 3, preceded by *Cla97C11G210270* auxin-responsive protein SAUR21 and SRK2H protein kinase *Cla97C04G069000*. The downregulated genes were mostly auxin responsive and classified into different subgroups. Members of the GH3 family, including *Cla97C05G096220* and

Cla97C01G016350, exhibited reduced expression followed by multiple auxin-responsive family genes *Cla97C05G104280, Cla97C09G170160, Cla97C06G119700,* and *Cla97C08G156790* that were also suppressed. Similarly key transcription factors involved Cla97C02G044480 (bZIP TF), Cla97C01G011610 (TGA9 TF) Cla97C02G048210 (ERF factor) and *Cla97C02G044480* auxin responsive protein SAUR71 were suppressed. The other downregulated gene families involved C*la97C02G034050* Pathogenesis related protein-1, *Cla97C04G069570* protein kinase and *Cla97C11G212910, Cla97C10G205730* from abscisic acid receptor PYL4.

3.8. Protein Processing in endoplasmic reticulum.

The protein processing in endoplasmic reticulum pathway involved around twenty-four genes among which four genes were downregulated, and twenty genes were upregulated for autotetraploid watermelon line K5M 4x female flower (Fig. 3J). The genes with decreased expression levels involved *Cla97C01G001870* belonging to SEC61-alpha family followed by *Cla97C06G126340, Cla97C11G223450, Cla97C08G157760* belonging to heat shock protein family. The genes with upregulation were *Cla97C04G074210, Cla97C11G217390* belonging to alpha-1,2-Mannosidase, and HSP 70, followed by *Cla97C01G000110, Cla97C07G132310, Cla97C07G132180, Cla97C10G191220, Cla97C01G006780, Cla97C04G071950, Cla97C05G-108440, Cla97C07G132280, Cla97C07G132220, Cla97C07G132150, Cla97C03G051930* and *Cla97C10G187290, Cla97C05G099440* genes belonging to HSP 20 gene family that were also upregulated. Similarly, *Cla97C07G132190* gene from endoplasmin homolog followed by *Cla97C09G172860* belonging to class II heat shock protein, Cla97C02G033390, Cla97C07G132-*300* members of small heat shock protein family and *Cla97C08G145950* gene containing UBX domain- protein also displayed elevated expression. The genes with upregulation were *Cla97C04G074210, Cla97C11G217390* belonging to alpha-1,2-Mannosidase, and heat shock protein 70, followed by *Cla97C01G000110, Cla97C07G132310, Cla97C07G132180, Cla97C10-G191220, Cla97C01G006780, Cla97C04G071950, Cla97C05G108440, Cla97C07G132280,* and *Cla97C07G132220, Cla97C07G132150, Cla97C03G051930, Cla97C10G187290, Cla97C05G0-99440* genes belonging to HSP 20 gene family were also upregulated. Similarly, *Cla97C07G132190* gene from endoplasmin homolog followed by *Cla97C09G172860* belonging to class II heat shock protein, *Cla97C02G033390, Cla97C07G132300* members of small heat

shock protein family and *Cla97C08G145950* gene containing UBX domain- protein also displayed elevated expression.

For the female flower 2 DAP in the autotetraploid watermelon line K5M 4x there were twenty-seven genes that were downregulated (Fig. 3K). The small heat shock protein (HSP20) family had seventeen genes that were suppressed along with Cla97C01G006780 UBX domain-containing protein and three Cla*97C05G108440, Cla97C01G000110* chloroplastic small heat shock proteins were also downregulated. The (HSP70) heat shock protein family had *Cla97C09G181360, Cla97C09G181410, Cla97C11G217390* genes also displayed reduced expression. The remaining heat shock proteins *Cla97C03G067590, Cla97C09G172860,* followed by DNA J protein homolog *Cla97C03G062120* and *Cla97C05G099440* from class II heat shock protein were also downregulated in their expressions.

3.9. Brassionsteroid Pathway

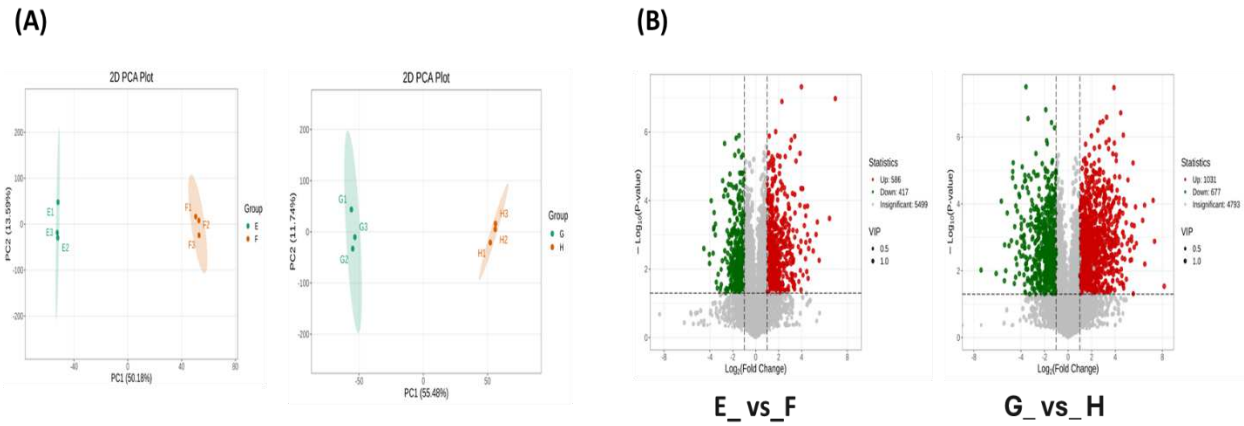
For the female flower 2 DAP in the autotetraploid watermelon line K5M 4x four genes were involved in which two genes Cla97C07G140940, Cla97C07G140960 from Cytochrome P450 71A1 protein were repressed followed by Cla97C09G180900, Cla97C11G209280 genes that were elevated for their expressions (Fig. 3M).

3.10. Assessment of the DEGs by qRT-PCR

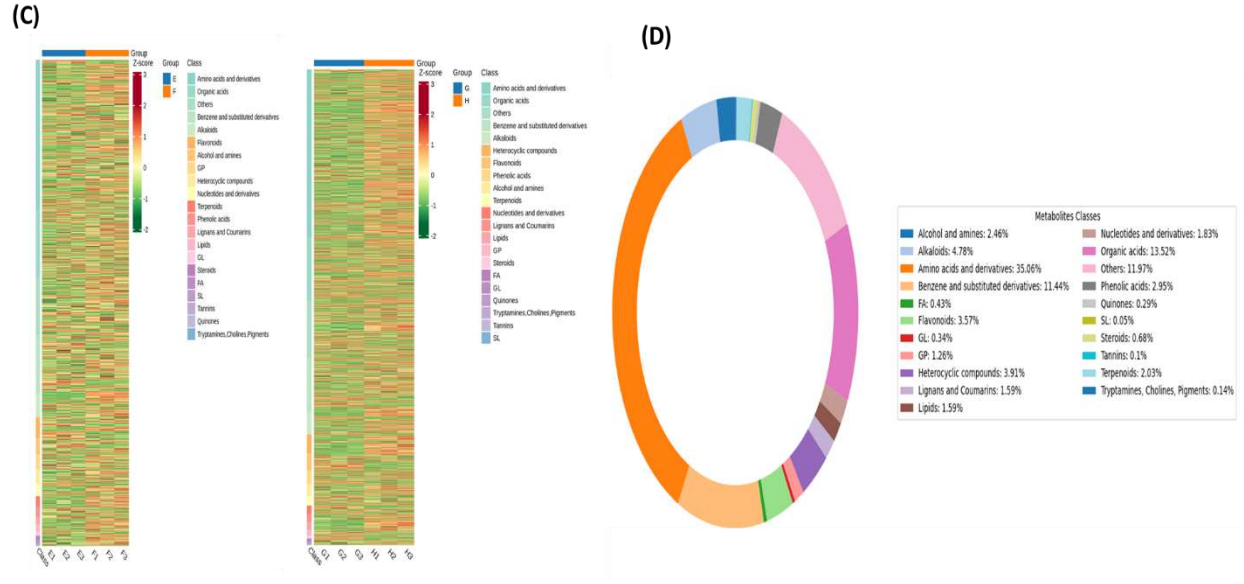
To assess the RNA seq results and differentially expressed genes we identified twelve genes from 1DAP female flower followed by ten genes taken from the female flower (Fig. 3N). For the 1DAP samples four genes were identified from phenylpropanoid biosynthesis pathway followed by four genes selected from plant hormone signal transduction pathway and four genes from protein processing in endoplasmic reticulum. Among all the genes six genes were upregulated, six genes were suppressed and qPCR results were consistent with their subsequent RNA seq data. The genes involved for 2DAP samples had two genes from brassionsteroid biosynthesis pathway preceded by four genes from plant hormone signal transduction pathway and four genes from protein processing in endoplasmic reticulum. Among them all the genes were significantly downregulated, and their qPCR expression was aligned with transcriptome data.

3.11. Differences in metabolites among diploid and autotetraploid watermelon female ovaries after 1 DAP and 2DAP.

The nontarget metabolome analysis was used to identify the key metabolites linked with key pathways responsible for ovule development in female flower samples after 1DAP and 2 DAP. The QC control analysis for the sample quality verification of metabolome samples revealed tightly clustered in the principal component analysis (PCA) for (E-Vs-F) and (G-vs-H) (Fig. 4A). The metabolome volcano plots for 1DAP female flower samples revealed 586 upregulated and 417 downregulated metabolites (Table S4), followed by 1031 elevated and 677 suppressed (Table S5), for the female flower samples at 2DAP (Fig. 4B). The heat maps revealed differential clustering of metabolites across different classes among the samples (Fig. 4C). The metabolites were labelled into different subcategories involving amino acids and derivatives (35.06 %) followed by organic acids (13.52 %), Benzene and substituted derivatives (11.44%) Others (11.97%), alcohol and amines (2.46%), alkaloids (4.78%) Fatty acids (0.43%), Flavonoids (3.7%), GL (0.34%), GP (1.26%), Heterocyclic compounds (3.91%), Lignans and Coumarins (1.59%), Lipids (1.59%), Nucleotides and derivatives (1.83%), Phenolic acids (2.95%), Quinones (0.29%), SL(0.05%) steroids (0.68 %), Tannins (0.1%), Terpenoids (2.03%) and Tryptamines (0.14%) respectively(Fig. 4D).The KEGG pathways analysis for metabolites among 1DAP female flowers for (E-Vs-F) enriched Polyketide sugar unit biosynthesis followed by phenylalanine, tryptophan, tyrosine biosynthesis, Tyrosine metabolism, biosynthesis of secondary metabolites, and Indole alkaloid pathway as the top five significantly enriched pathways(Fig. 4E).Similarly, for 2 DAP female flower (G-vs-H) samples the significantly enriched top five pathways involved tropane, piperidine and pyridine alkaloid biosynthesis, Amino acyl tRNA biosynthesis, Tryptophan metabolism, Indole alkaloid pathway and biosynthesis of secondary metabolites. (Fig. 4F).

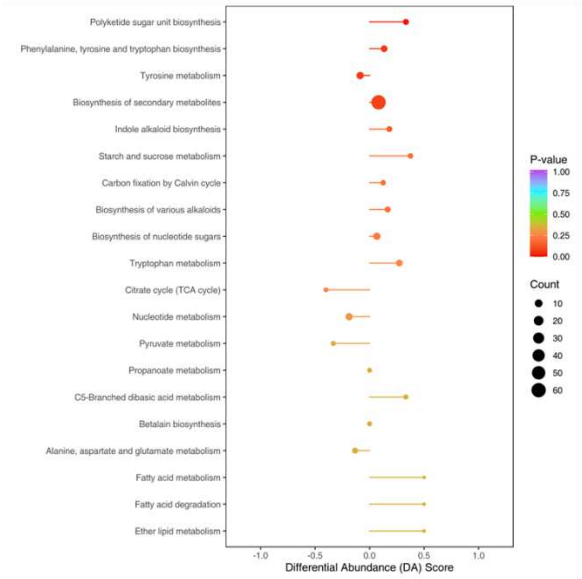

(A)
2D PCA Plot
PC1 (50.18%)
PC2 (13.59%)
Group
E
F
2D PCA Plot
PC1 (55.48%)
PC2 (11.74%)
Group
G
H
(B)
Statistics
Up: 586
Down: 417
Insignificant: 5499
VIP
0.5
1.0
Log2(Fold Change)
−Log10(P-value)
E_ vs_F
Statistics
Up: 1031
Down: 677
Insignificant: 4793
VIP
0.5
1.0
Log2(Fold Change)
−Log10(P-value)
G_ vs_H

483


(C)
Group
Z-score
Group
Class
E
F
Amino acids and derivatives
Organic acids
Others
Benzene and substituted derivatives
Alkaloids
Flavonoids
Alcohol and amines
GP
Heterocyclic compounds
Nucleotides and derivatives
Terpenoids
Phenolic acids
Lignans and Coumarins
Lipids
GL
Steroids
FA
SL
Tannins
Quinones
Tryptamines,Cholines,Pigments
Class
E1
E2
E3
F1
F2
F3
Group
Z-score
Group
Class
G
H
Amino acids and derivatives
Organic acids
Others
Benzene and substituted derivatives
Alkaloids
Heterocyclic compounds
Flavonoids
Phenolic acids
Alcohol and amines
Terpenoids
Nucleotides and derivatives
Lignans and Coumarins
Lipids
GP
Steroids
FA
GL
Quinones
Tryptamines,Cholines,Pigments
Tannins
SL
Class
G1
G2
G3
H1
H2
H3
(D)
Metabolites Classes
Alcohol and amines: 2.46%
Alkaloids: 4.78%
Amino acids and derivatives: 35.06%
Benzene and substituted derivatives: 11.44%
FA: 0.43%
Flavonoids: 3.57%
GL: 0.34%
GP: 1.26%
Heterocyclic compounds: 3.91%
Lignans and Coumarins: 1.59%
Lipids: 1.59%
Nucleotides and derivatives: 1.83%
Organic acids: 13.52%
Others: 11.97%
Phenolic acids: 2.95%
Quinones: 0.29%
SL: 0.05%
Steroids: 0.68%
Tannins: 0.1%
Terpenoids: 2.03%
Tryptamines, Cholines, Pigments: 0.14%

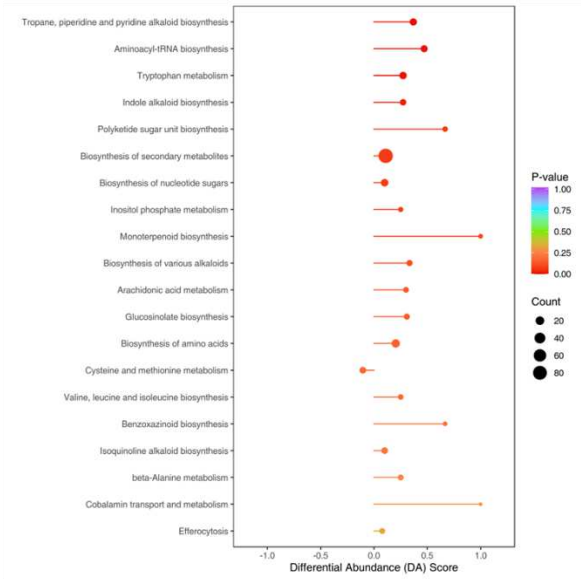
484

(E)



E_ vs_F Female Flower 1DAP

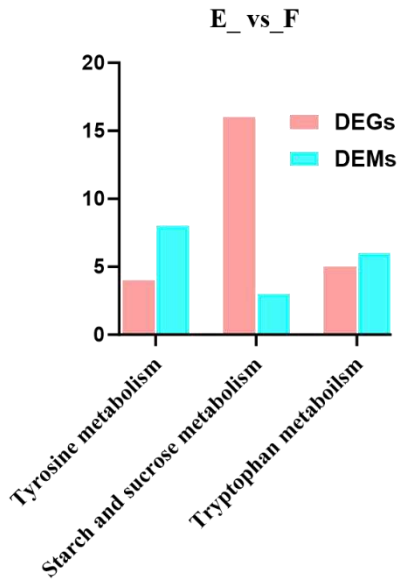
(F)



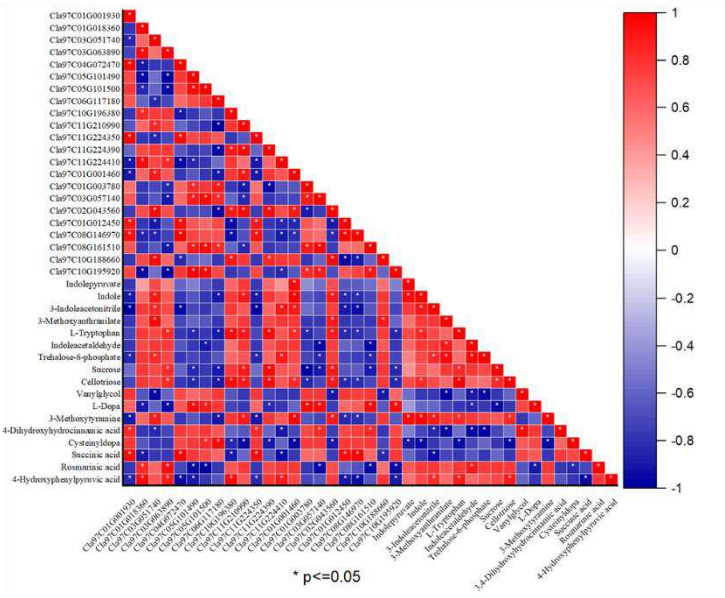
G_ vs_H Female flower 2DAP

485

(G)



(H)



486

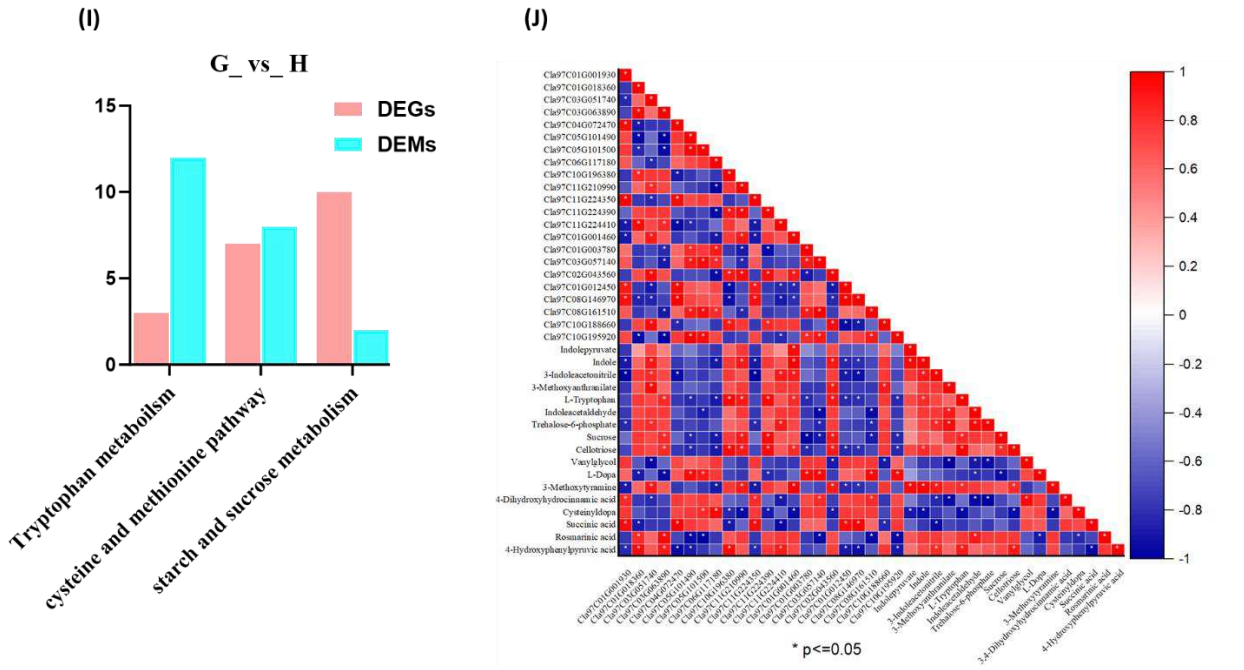


Figure 4. Integrated transcriptomic and metabolomic analyses of female flowers at different 1DAP and 2DAP. (A) Principal component analysis (PCA) of transcriptomic and metabolomic profiles showing clear separation between groups E vs. F (PC1: 39.5%, PC2: 20.5%) and G vs. H (PC1: 54.6%, PC2: 18.4%). (B) Volcano plots of differentially expressed genes (DEGs) and metabolites (DEMs) in E vs. F and G vs. H, highlighting upregulated, downregulated, and stable features. (C) Heatmaps of expression patterns for DEGs and DEMs across samples, illustrating stage-specific clustering. (D) Classification of metabolites into major biochemical categories, represented as a donut chart with relative percentages. (E–F) KEGG Pathway enrichment analyses for E vs. F (Female Flower 1DAP) and G vs. H (Female Flower 2DAP), showing significantly enriched metabolic pathways. (G–I) Comparative bar charts of DEGs and DEMs involved in key pathways (tyrosine metabolism, starch and sucrose metabolism, tryptophan metabolism, cysteine and methionine metabolism) across E vs. F and G vs. H. (H, J) Correlation matrix heatmaps of metabolites, with positive and negative associations indicated by color gradients and statistical significance ($p < 0.05$) marked by asterisks.

3.12. Differentially Expressed Metabolites (DEM) linked to Enriched Pathways

The KEGG pathways for 1DAP female flowers (E-Vs-F) involved tyrosine metabolism, sugar and sucrose metabolism and tryptophan metabolism. The tyrosine pathway involved eight different metabolites that included vanylglycol, L-Dopa, 3,4-Dihydroxyhydrocinnamic acid, cysteinyl dopa and succinic acid that were suppressed followed by 3-methoxytyramine, Rosmarinic acid and 4-hydroxyphenylpyruvic acid that were upregulated, Similarly sugar and sucrose metabolism had three metabolites trehalose-6-phosphate, sucrose and cellotriose that were elevated in their

expression. The tryptophan metabolism had six metabolites based on indole pyruvate, indole, 3-indoleacetonitrile, 3-methoxyanthranilate, L-Tryptophan and indole acetaldehyde that were upregulated.

The KEGG pathways for 2DAP female flower (G-vs-H) had tryptophan, cysteine and methionine pathway and starch and sucrose metabolism. The tryptophan metabolism contained twelve metabolites among which Formyl anthranilic acid, 5-hydroxyindoleacetic acid, Indole-3-acetamide with suppressed expression and Indole, 2-Aminobenzoic acid, 5-hydroxy-L-tryptophan, 3-Indoleacetonitrile, Xanthurenic acid, Serotonin, 3-Methylindole, L-Tryptophan, Indole acetaldehyde and 5-Hydroxyindoleacetic acid were up regulated. The cysteine and methionine enriched pathway displayed eight metabolites including phosphoserine, S-(5-Adenosy)-L-Homocysteine, O-Succinyl-L-Homoserine, 5'-Deoxy-5'-(Methylthio) Adenosine followed by 3-(Methylthio)propionic acid that were suppressed while S-Inosyl-L-homocysteine, L-Homoserine and Methionine were upregulated. The starch and sucrose metabolism involved D-Fructose-6-phosphate that was suppressed followed by Glucose which presented elevated expression.

3.13. Integration of Gene Expression and Metabolic Pathways for female flowers at 1DAP and 2 DAP.

To understand the intergenic interaction along with key metabolites involved in different highly enriched pathways for ovule development at 1 DAP (E-Vs-F) and 2 DAP (G-vs-H) an integrated transcriptome and metabolomic analysis was carried out. The integrative analysis for the 1 DAP samples revealed around four genes involved Tyrosine metabolism with eight different metabolites followed by starch and sucrose pathway linking thirteen genes with three metabolites and tryptophan metabolism had five genes interacting with six different metabolites (Fig. 4G). The tryptophan metabolism pathway had *Cla97C01G001460* significantly positively correlation with L-Dopa, Rosmarinic acid followed by *Cla97C03G057140* for Cysteinyldopa, *Cla97C01G003780* with 3-Methoxytyramine and *Cla97C02G043560* linked with 4-Hydroxyphenylpyruvic acid. Similarly strong negative correlation existed between *Cla97C01G001460* and Succinic acid succeeded by Cla97C01G003780 with Vanylglycol and *Cla97C03G057140* with 3,4-Dihydroxyhydrocinnamic acid (Fig. 4H). The starch and sucrose metabolism revealed significantly strong positive correlation for *Cla97C01G001930, Cla97C01G018360* with sucrose, Trehalose-6-phosphate followed by *Cla97C03G051740* associated with sucrose and *Cla97C03G063890* linked with cellotriose. The negative correlation existed for

Cla97C05G101490 with Trehalose-6-phosphate followed by *Cla97C06G117180* for sucrose and *Cla97C11G224350* associated with cellotriose (Fig. 4H). The Tryptophan metabolism involved *Cla97C01G012450* significantly corelated with indolepyruvate, and indole followed by *Cla97C08G146970* positively corelated with L-Tryptophan and *Cla97C10G188660* positively linked with indole acetaldehyde. Similarly, *Cla97C10G195920* was negatively correlated with Indolepyruvate followed by negative correlation for Cla*97C08G161510* with 3-Indoleacetonitrile (Fig. 4H).

The integrated analysis for 2 DAP involved 3 genes and twelve different metabolites followed by cysteine and methionine pathway with seven genes and eight metabolites and starch and sucrose metabolism having only 2 metabolites and ten genes (Fig. 4I). The tryptophan metabolism had *Cla97C02G030540* strong positive correlation with L-Tryptophan and Formyl anthranilic acid followed by *Cla97C02G030550* positively corelated with 5-hydroxy-L-tryptophan and Indole-3-acetamide and *Cla97C08G161510* positively correlated to serotonin and Xanthurenic acid. A strong negative correlation existed for *Cla97C02G030540* gene with 3-Methylindole, followed by Cla97C02G030550 negatively associated with Indole acetaldehyde and *Cla97C08G161510* negatively correlated to 5-Hydroxyindoleacetic acid and 2-Aminobenzoic acid (Fig. 4J). The cysteine and methionine pathway composed of *Cla97C03G066540, Cla97C10G185400* and *Cla97C01G017090* genes positively corelated with Methionine, S-(5-Adenosyl)-L-Homocysteine and O-Succinyl-L-Homoserine respectively While negative correlation had occurrence for *Cla97C09G173910, Cla97C11G223810, Cla97C02G043560* genes negatively corelated to 3-(Methylthio)propionic acid, 5'-Deoxy-5'-(Methylthio) Adenosine and Phosphoserine Lastly the starch and sucrose metabolism had *Cla97C03G063770, Cla97C06G117180* gene positively corelated to glucose and D-Fructose-6-phosphate while two other genes *Cla97C05G086630* and *Cla97C02G027410* were negatively corelated to these metabolites. (Fig. 4J).

4.0 Discussion

4.1. Polyploidy influences pollen–pistil interactions in watermelon

The contrasting pollen–pistil interactions between diploid and autotetraploid K5M watermelon underscore key reproductive limitations imposed by polyploidization. Efficient germination, rapid elongation, and dense pollen tube growth in the diploid line reflect coordinated tip polarity and effective stylar guidance, facilitating successful fertilization (Higashiyama & Yang, 2017). In

contrast, the autotetraploid exhibits delayed germination, reduced elongation, and pronounced structural abnormalities, indicative of disrupted polarity control. These defects likely arise from perturbations in calcium signaling, cell wall dynamics, and cytoskeletal organization, all essential for polarized tip growth (Cheung & Wu, 2008). Polyploid plants often exhibit compromised reproductive capacity by reduction of pollen fertility, abnormal pollen tube germination, impaired pollen tube growth resulting in reducing fertilization and resulted in decreased seed yields (Sattler et al., 2016). Similar abnormalities associated with pollen development, pollen germination, and pollen tube progression have also been observed across many polyploid crops involving banana (Severyns et al.,2025) apple (Adachi et al., 2009), rice (Li et al.,2017) and Arabidopsis (Westermann et al., 2024). Overall, the delayed, sparse, and structurally abnormal pollen tube growth observed in autotetraploid watermelon reflects impaired pollen-pistil communication and reduces transmission efficiency. These phenotypic variations might be associated with decreased fertilization efficiency resulting in reduced fertility associated with autotetraploidy.

4.2. Ovule development was impaired in autotetraploid watermelon.

Ovule development following fertilization is central to seed set, and the present results indicate that ploidy variation imposes a clear limitation in autotetraploid watermelon. Histological observations, together with seed counts, showed that diploid ovaries produced a greater number of well-organized and rapidly expanding ovules at both 1 and 2 DAP. In contrast, autotetraploid ovaries displayed delayed growth and reduced structural integrity. Although ovule development progressed in both ploidies, its rate and consistency were markedly higher in diploids, suggesting that early post-pollination stages represent a critical bottleneck in autotetraploids. Comparable patterns have been reported in other polyploid systems, including rice (Ku et al., 2022), where disruptions in reproductive processes reduce seed set. Similar reductions in female fertility have also been documented in Arabidopsis and Brassica (Comai, 2005; Ramsey and Schemske, 2002). Together, these findings suggest that impaired early ovule development contributes substantially to reduced reproductive efficiency in autotetraploid watermelon.

4.3. Elevated antioxidant enzyme activities facilitate oxidative stress mitigation.

The present results indicate a ploidy-dependent enhancement of antioxidant metabolism during early post-pollination development. At 1 and 2 DAP, autotetraploid ovary tissues showed higher activities of CAT, SOD, PPO, and POD compared with diploids, suggesting a stronger redox

buffering capacity. Elevated antioxidant activity during these stages likely reflects the increased metabolic demand associated with pollen–pistil interactions, fertilization, and early ovule development. Similar trends have been reported in other polyploid crops, including Brassica and citrus species (Sudo et al., 2021; Shi et al., 2020). The progressive rise in enzyme activity from 1 to 2 DAP across both ploidies indicates a coordinated intensification of ROS-scavenging mechanisms during ovule maturation. Notably, POD activity was comparatively higher, suggesting a key role in hydrogen peroxide detoxification and cell wall modification during tissue differentiation (M. F. Ali et al., 2024). Increased SOD and CAT activities further support maintenance of redox homeostasis, in both Arabidopsis and cereal crop species which was essential for their reproductive success (Kaya et al., 2014).

4.4. Phenylpropanoid pathway enhances stress resilience.

The phenylpropanoid pathway plays a significant role in plant development, structural integrity, and stress adaptation. In the present study, the upregulation of caffeic acid 3-O-methyltransferase (COMT) and cinnamoyl-CoA reductase (CCR) suggests enhanced monolignol biosynthesis, a key step in lignin formation. Similar induction of these genes has been linked to increased lignification in crops such as maize, where disruptions in associated pathways lead to developmental defects (Qi et al., 2016). Increased lignin deposition is known to strengthen cell walls, thereby improving resistance to lodging and pathogen attack, as reported in wheat (Riaz et al., 2023). In addition, elevated expression of cytochrome P450 84A1-like genes indicates active lignin modification through ferulate-5-hydroxylase activity, contributing to syringyl lignin synthesis. This process is essential for maintaining cell wall stability under stress conditions and has been widely reported in Arabidopsis and other crops (Meyer et al., 1996; Riaz et al., 2023). The concurrent upregulation of peroxidase genes further supports enhanced lignin polymerization and regulation of oxidative stress through hydrogen peroxide metabolism (Yang et al., 2023). The increased activity of antioxidant enzymes (CAT, SOD, PPO, and POD) observed here suggests a coordinated response balancing reactive oxygen species as both signaling molecules and potential cellular stressors. Conversely, the downregulation of vinorine synthase implies a shift in metabolic allocation away from alkaloid biosynthesis toward structural defense. Such trade-offs have been observed in crops under stress, including cotton and apple (Zhang et al., 2023; Yang et al., 2023). Collectively, these

findings point to a coordinated transcriptional adjustment favoring lignification and redox homeostasis to enhance stress resilience.

4.5. Plant hormone signaling controls fertility

Autopolyploidization in the watermelon line K5M 4x markedly reshaped plant signal transduction pathways at 1 day after pollination (DAP), primarily through suppression of hormone-associated gene networks. Auxin-responsive genes were the most prominently affected, followed by components of the ethylene pathway, both of which play central roles in plant growth and development (Li Bao et al., 2024). The coordinated downregulation of key auxin-responsive families including Aux/IAA, Small Auxin Up RNA (SAUR), and GH3 revealed disruption of early post-pollination developmental programs. Reduced expression of SAUR21-like and SAUR50-like genes may limit ovule enlargement and integument expansion during early fruit set. Aux/IAA and SAUR gene families regulate cell elongation through modulation of H^{+-}ATPase activity and cell wall loosening; their suppression at 1 DAP is therefore consistent with reduced cell expansion and aligns with the observed decrease in ovule size and number (Spartz et al., 2012; Bao Ying et al., 2024). Concurrently, altered GH3 gene expression indicated enhanced auxin conjugation, suggesting a buffering mechanism that fine-tunes intracellular auxin levels during floral and ovule development (Staswick et al., 2005). In contrast, the ethylene signaling pathway was activated, as evidenced by upregulation of an ethylene-responsive transcription factor (ERF1B) and a protein kinase. Ethylene is a key regulator of developmental transitions, including fruit initiation, and often acts antagonistically to auxin (Han et al., 2024). The induction of ERF1B and associated signaling components supported a model in which ethylene auxin crosstalk coordinates reproductive differentiation (Stepanova & Alonso, 2009). Additionally, downregulation of a bZIP transcription factor, a histidine-containing phosphotransfer protein, and an abscisic acid (ABA) receptor indicates concurrent modulation of ABA and cytokinin signaling pathways.

By 2 DAP, the hormonal landscape exhibited a distinct shift characterized by partial restoration of auxin-associated processes. Upregulation of auxin-responsive SAUR21 and the SnRK2-type kinase SRK2H suggested enhanced auxin transport and signaling. Local auxin accumulation is essential for ovule primordia development, as demonstrated in Arabidopsis (Benková et al., 2003). Increased SAUR21 expression was consistent with its role in cell wall loosening, ovary expansion, and early fruit initiation, as well as its broader involvement in developmental and stress responses

(Ren and Gray, 2015; Yan et al., 2023). The induction of SRK2H further suggests integration between auxin and ABA signaling pathways, reflecting coordinated developmental regulation (Fujii et al., 2009). Despite this partial recovery, repression of TGA and bZIP transcription factors persisted, indicating continued modulation of transcriptional networks governing hormone crosstalk (Gatz, 2013). Furthermore, downregulation of the ABA receptor PYL4 suggests reduced ABA perception. ABA receptors of the PYR/PYL family regulate seed and ovule development through SnRK2-mediated signaling (Park et al., 2009) and their suppression is consistent with the antagonistic relationship between ABA and auxin during fruit set. Overall, these findings demonstrate that autotetraploidy in watermelon K5M 4x triggers dynamic, stage-specific reprogramming of hormonal signaling pathways, underpinning altered ovule development and fruit set efficiency.

4.6. Endoplasmic Reticulum: Central Hub of Protein Folding and Processing

To maintain proteostasis following genome doubling, the autotetraploid watermelon line K5M 4x exhibited dynamic regulation of the endoplasmic reticulum (ER) protein processing pathway during early reproductive development. At 1 day after pollination (DAP), 24 genes associated with ER protein processing were differentially regulated, indicating a coordinated response to proteotoxic stress imposed by polyploidization. Notably, suppression of SEC61A, linked with translational protein responsible for protein import into the ER lumen, revealed attenuation of bulk secretory flux. This reduction may serve to alleviate ER burden under conditions of increased protein-folding demand, thereby maintaining cellular homeostasis during ovary development (Wang et al., 2021). Concurrently, multiple heat shock protein (HSP) family members, including HSP20, HSP70, and other small HSPs, were strongly upregulated. These molecular chaperones play essential roles in protein folding, stabilization, and degradation. HSP20 proteins act as holdase chaperones, preventing aggregation of misfolded proteins and stabilizing partially folded intermediates, thereby enhancing cellular stress tolerance. Small HSPs have been widely implicated in reproductive stability and stress resilience, including roles in male fertility regulation under heat stress conditions in crops such as grasses and cotton (Khan et al., 2022). Similarly, HSP70 family members contribute to reactive oxygen species (ROS) homeostasis and reproductive development under stress (Dan Luo et al., 2023). The elevated expression of these chaperones suggests an expanded buffering capacity to counteract proteotoxic stress in the autotetraploid

ovary. In addition to chaperone induction, increased expression of α-1,2-mannosidase genes highlight enhanced ER quality control mechanisms. These enzymes are central to glycoprotein processing and ER-associated degradation (ERAD), facilitating the removal of mannose residues from misfolded glycoproteins and targeting them for degradation. This glycan-dependent surveillance system ensures fidelity in protein maturation and trafficking through the secretory pathway (Fregno et al., 2021).

By 2 DAP, a marked shift in proteostasis regulation was observed, with twenty-seven genes significantly downregulated, indicating suppression of ER and cytosolic protein quality control machinery. This included coordinated repression of HSP20 and HSP70 family members, suggesting reduced reliance on chaperone-mediated folding as developmental programs progressed. The clustered genomic distribution of HSP20 genes raises the possibility of coordinated transcriptional or epigenetic regulation, consistent with observations in cucurbit species (Wang et al., 2021). Similar downregulation of chaperone systems during reproductive transitions has been reported in Arabidopsis, rice, and maize, where precise temporal control of proteostasis was required for gametophyte and embryo development (Sun et al., 2002; Sarkar et al., 2009).

These stage-specific dynamics may reflect gene dosage effects associated with polyploidy, leading to altered transcriptional regulation and chromatin accessibility (Feng et al., 2022). Collectively, the transient upregulation of ER-associated chaperones at 1 DAP, followed by their suppression at 2 DAP, suggests a tightly regulated proteostasis program essential for early reproductive development in autotetraploid watermelon.

4.7. Brassinosteroid Signaling in Plant Fertility

BRs, which are steroidal phytohormones, were required to control the growth of plants, differentiation of reproductive organs, and ovule development in complex biosynthetic and signaling pathways that are mainly mediated by cytochrome P450 enzymes. These enzymes are involved in catalyzing oxidation reaction, which regulate the formation and maintenance of active BR intermediates and these mediate floral organ development and fertility (Wang et al., 2006). The autotetraploid watermelon line K5M 4x revealed the suppression of two genes and upregulation of two other genes belonging to cytochrome P450 gene family. The role of cytochrome P450 in BR biosynthesis and metabolic degradation, BR metabolic control, and hormone homeostasis

CYP450 enzymes are essential components that may be directly impacted through transcriptional regulation in reproductive development (Ohnishi et al., 2012). The downregulation of CYP71A1-related genes displayed the suppression of BR synthesis flux in the ovary development whereas the elevation levels of some genes might be serving as a compensatory resource to retain hormonal balance for ovule differentiation. Previously it had been observed that disruption of BR synthesis associated with impaired gynoecium and ovule development suggesting role of BR synthesis pathways for reproductive development (Zu et al., 2022).

4.8. Metabolome and transcriptome dynamics in ovule development

Ovule development in the female ovary was a highly coordinated process involving integrated gene networks and metabolic pathways, as revealed by combined transcriptomic and metabolomic analyses at 1 and 2 days after pollination (DAP). Key pathways contributing to this process included tryptophan, tyrosine, starch and sucrose, as well as cysteine and methionine metabolism. On 1 DAP, starch and sucrose metabolism showed strong positive correlations between *Cla97C01G001930 and Cla97C01G018360* with sucrose and trehalose-6-phosphate, indicating tight regulation of carbohydrate flux during early developmental transitions. Similar roles of sucrose metabolism in supporting seed development have been reported in *Akebia trifoliata* (Liu et al., 2024). Consistently, sugar metabolism was known to influence seed vigor and stress responses, underscoring its broader developmental significance (Yang et al., 2023; Lu et al., 2023). In parallel, strong gene–metabolite correlations in tyrosine and tryptophan pathways suggested active regulation of aromatic amino acid-derived secondary metabolism during early ovule differentiation. Genes such as Cla97C01G001460, Cla97C03G057140, Cla97C01G003780 were positively associated with metabolites including L-DOPA, rosmarinic acid, cysteinyldopa, reflecting enhanced phenolic and indole pathway activity. These metabolites contribute to signaling, defense, and redox homeostasis during reproductive tissue differentiation (Tohge et al., 2013). Moreover, the presence of indole intermediates supports modulation of auxin biosynthesis, as tryptophan-dependent pathways were primary sources of indole-3-acetic acid (IAA), a key regulator of ovule initiation and gametophyte development (Zhao, 2012; Ceccato et al., 2013).

By 2 DAP, metabolic reprogramming became more pronounced, with tryptophan metabolism central to the production of auxin-related and indole-derived compounds. Genes such as *Cla97C02G030540, Cla97C02G030550, Cla97C08G161510* showed positive correlations with

metabolites including tryptophan derivatives, serotonin, and xanthurenic acid, indicating enhanced synthesis of indole alkaloids and phytohormone precursors (Chang et al., 2024). Concurrently, cysteine and methionine metabolism emerged as key pathways, with metabolites such as methionine, S-adenosyl-L-homocysteine, and O-succinyl-L-homoserine correlating with specific gene modules. This shift reflects increased demand for sulfur-containing compounds, methyl donors, and redox regulators essential for cellular differentiation and growth, consistent with observations in sesame seed development (Zhang et al., 2025). Overall, these findings highlight coordinated metabolic reprogramming underlying ovule development

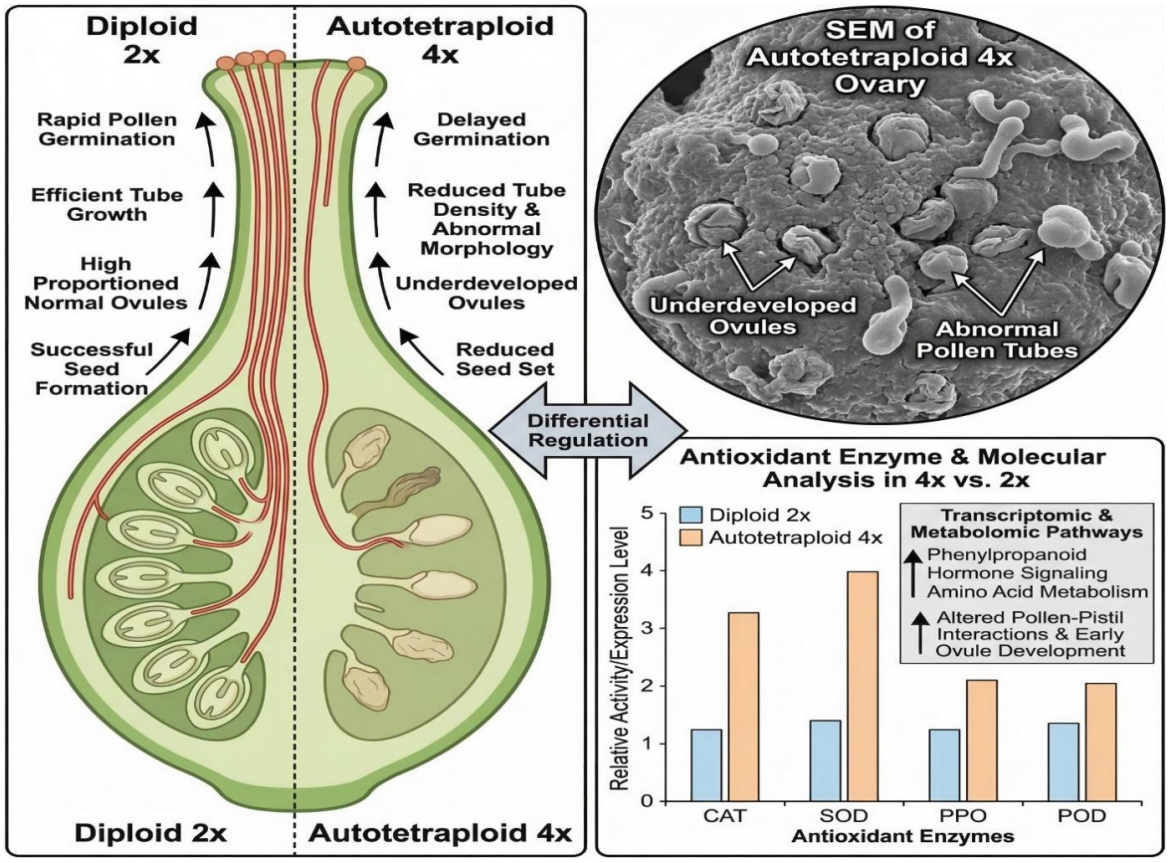


Figure 5. Schematic illustration of postpollination pistil interactions associated with female fertility impacted by polyploidization in autotetraploid watermelon.

5. Conclusion

This study provides the first comprehensive multi-omics investigation for female reproductive abnormalities in autotetraploid watermelon line K5M 4x relative to its diploid counterpart K5M 2x. Scanning electron microscopy revealed that autotetraploidy severely affects pollen–pistil interactions through later germination, decreased pollen tube density, and structural abnormalities, collectively reducing fertilization efficiency. Histological analysis confirmed these defects resulted in reproductive failure, with autotetraploid ovaries exhibiting higher proportions of underdeveloped ovules and lower seed set. Increased antioxidant enzyme activities suggests elevated oxidative stress and metabolic burden might be linked to genome doubling. Transcriptomic analysis revealed differential regulation of phenylpropanoid biosynthesis, hormone signal transduction, endoplasmic reticulum protein processing, and brassinosteroid biosynthesis pathways. Suppression of auxin-responsive gene families including Aux/IAA, SAUR, and GH3 devise impaired ovule expansion and integument development. Metabolomic profiling identified reprogramming of tryptophan, tyrosine, cysteine, methionine, and sucrose metabolism, highlighting disrupted auxin precursor synthesis and carbohydrate allocation during ovule differentiation. Collectively, autotetraploidy might reshapes the transcriptional and metabolic landscape of watermelon female ovaries, providing a foundational framework for improving seed production efficiency in triploid seedless watermelon breeding.

Declaration of conflict of interest

The authors declare no conflict of interest.

Abbreviations

DAP	Days after pollination
GAs	Gibberellins
CKs	Cytokinins
ABA	Abscisic Acid
JAs	Jasmonates
ROS	Reactive oxygen species
POD	Peroxidase
PPO	Polyphenol oxidase
SOD	Superoxidase dismutase

CAT Catalase

RNA-seq Ribonucleic Acid Sequencing

DEGs Differentially expressed genes

GO Gene ontology

KEGG Kyoto Encyclopedia of Genes and Genomes

HAP Hours after pollination

DEMs Differentially expressed metabolite.

NCBI National Center for Biotechnology Information

SRA Sequence Read Archive

Ethics approval and consent to participate

The seeds of varietal lines K5M 2x and K5M 4x were provided by polyploidy watermelon team from Zhengzhou Fruit Research Institute, CAAS, Zhengzhou, China. The experimental work involving plant specimens adhered to all relevant institutional, national, and international standards and regulatory requirements. Since no human or animal subjects were used in this study, approval from an ethics committee and informed consent were not mandatory.

Consent for publication

All the participating authors have approved the manuscript for publication.

Availability of data and materials

RNA-seq data generated in this study from the watermelon cultivars K5M 2x and K5M4x female flowers at 1 DAP and 2DAP developmental stages were deposited in the NCBI Sequence Read Archive (SRA) under Bio Project PRJNA1490325. Besides that, all the data including DEGs, Gene primers and DEMs data has been provided in supplementary files.

Competing Interests

All the authors declare no conflict of interest.

Funding sources

This work was granted by Henan Province Key Research and Development Program (241111521500), the National Natural Science Foundation of China (32502725), Agricultural Science and Technology Innovation Program (CAAS-ASTIP-2025-ZFRI), (CARS-25-2025-G5).

Muhammad Zeeshan Sajjad carried out the investigation, curated the data, and wrote the original draft of the manuscript. **Xuqiang Lu** contributed to the methodology; **Eftekhar Mahmud** participated in the investigation and reviewed and edited the manuscript. **Fikru Tamiru Kenea** assisted with the investigation and software/data handling. **Mekonnen Tolasa Gonfa** contributed to the investigation and validated the results. **Yang Dongdong** assisted with data curation**. Chen Gang** performed formal analysis and prepared the visualizations**. Luo Xiaowen** contributed to the methodology and provided resources**. Nan He** reviewed and edited the manuscript. **Hongju Zhu** conceptualized the study, supervised the project, administered project resources, secured funding, and reviewed and edited the manuscript. **Wenge Liu** conceptualized the study, supervised the research, secured funding, and reviewed and edited the manuscript. All authors have read and approved the final version of the manuscript for publication.

Acknowledgments

The authors are grateful to Chinese Scholarship Council for the provision of generous scholarship grant for the leading author and fellow authors who participated in the research work. We extend our gratitude to Professor Liu Wenge and polyploidy watermelon group from Zhengzhou Fruit Research Institute, Henan, China for their generous guidance and feedback to improve research quality. The financial assistance for this work was allocated by Henan Province Key Research and Development Program, the National Natural Science Foundation of China, Agricultural Science and Technology Innovation Program and Agriculture Research System of China.

References.

Adachi, Y., Komori, S., Hoshikawa, Y., Tanaka, N., Abe, K., Bessho, H., Watanabe, M., & Suzuki, A. 2009. “Characteristics of fruiting and pollen tube growth of apple autotetraploid cultivars showing self-compatibility.” Journal of the Japanese Society for Horticultural Science, 78(4), 402–409. https://doi.org/10.2503/jjshs1.78.402

Ali, M. F., & Muday, G. K. 2024. “Reactive oxygen species are signaling molecules that modulate plant reproduction.” Plant, Cell & Environment, 47(5), 1592–1605. https://doi.org/10.1111/pce.14837

Bao, Y., Zou, Y., Huang, X., Rehman, M., Liu, C., Shi, S., Peng, D., Fahad, S., & Wang, B. 2024. “Genome-wide analysis and expression characteristics of small auxin-up RNAs genes in flax

(Linum usitatissimum L.).” Industrial Crops and Products, 217, 118874. https://doi.org/10.1016/j.indcrop.2024.118874

Baral, R., Vainer, A., Melzer, S., Hause, B., & Panda, S. 2025. “‘Bud to fruit’—hormonal interactions governing early fruit development”. Journal of Experimental Botany, 76(22), 6657–6673. https://doi.org/10.1093/jxb/eraf363

Benková, E., Michniewicz, M., Sauer, M., Teichmann, T., Seifertová, D., Jürgens, G., & Friml, J. 2003. “Local, efflux-dependent auxin gradients as a common module for plant organ formation”. Cell, 115(5), 591–602. https://doi.org/10.1016/S0092-8674(03)00924-3

Cai, M., Zeng, K., Li, L., et al. (2025). ROS homeostasis and cell wall biosynthesis pathway are involved in female inflorescence development of birch (Betula platyphylla). BMC Plant Biology, 25, 708. https://doi.org/10.1186/s12870-025-06740-2

Ceccato, L., Masiero, S., Sinha Roy, D., Bencivenga, S., Roig-Villanova, I., Ditengou, F. A., Palme, K., Simon, R., & Colombo, L. 2013. “Maternal control of PIN1 is required for female gametophyte development in Arabidopsis”. PLOS ONE, 8(6), e66148. https://doi.org/10.1371/journal.pone.0066148

Chang, Y., & Lv, G. 2024. “Key role of hormone signal transduction and lipid metabolism in the development of Nitraria sibirica leaves: An integrated metabolomic and transcriptomic analysis.” Industrial Crops and Products, 212, 118322. https://doi.org/10.1016/j.indcrop.2024.118322

Cheung, A. Y., & Wu, H. M. 2008. “Structural and signaling networks for the polar cell growth machinery in pollen tubes.” Annual Review of Plant Biology, 59, 547–572. https://doi.org/10.1105/tpc.106.047423

Comai, L. 2005. “The advantages and disadvantages of being polyploid”. Nature Reviews Genetics, 6(11), 836–846. https://doi.org/10.1038/nrg1711

Cui, Y., Ji, X., Zhang, Y., Liu, Y., Bai, Q., & Su, S. 2024. “Transcriptomic and metabolic profiling reveal the mechanism of ovule development in Castanea mollissima.” International Journal of Molecular Sciences, 25(4), 1974. https://doi.org/10.3390/ijms25041974

Duszynska, D., McKeown, P. C., Juenger, T. E., Pietraszewska-Bogiel, A., Geelen, D., & Spillane, C. 2013. “Gamete fertility and ovule number variation in selfed reciprocal F1 hybrid triploid plants

are heritable and display epigenetic parent-of-origin effects". New Phytologist, 198(1), 71–81. https://doi.org/10.1111/nph.12147

Feng, Z., Bi, Z., Fu, D., Feng, L., Min, D., Bi, C., & Huang, H. (2022). A comparative study of morphology, photosynthetic physiology, and proteome between diploid and tetraploid watermelon (*Citrullus lanatus* L.). *Bioengineering*, *9*(12), 746. https://doi.org/10.3390/bioengineering9120746

Food and Agriculture Organization of the United Nations (FAO 2024) FAOSTAT Statistical Database. https://www.fao.org/faostat/

Fregno, I., Fasana, E., Soldà, T., Galli, C., & Molinari, M. 2021. "N-glycan processing selects ERAD-resistant misfolded proteins for ER-to-lysosome-associated degradation". The EMBO Journal, 40(15), EMBJ2020107240. https://doi.org/10.15252/embj.2020107240.

Fujii, H., Chinnusamy, V., Rodrigues, A., Rubio, S., Antoni, R., Park, S. Y., Cutler, S. R., Sheen, J., Rodriguez, P. L., & Zhu, J. K. 2009. "In vitro reconstitution of an abscisic acid signalling pathway". Nature, 462(7273), 660–664. https://doi.org/10.1038/nature08599.

Gasser, C. S., Broadhvest, J., & Hauser, B. A. 1998. "Genetic analysis of ovule development". Annual Review of Plant Biology, 49(1), 1–24. https://doi.org/10.1146/annurev.arplant.49.1.1

Gatz, C. 2013. "From pioneers to collaborators: TGA transcription factors provide a molecular link between different stress pathways". Molecular Plant-Microbe Interactions, 26(2), 151–159. https://doi.org/10.1094/MPMI-04-12-0078-IA

Han, L., Wang, Z., Watkins, C. B., Ma, L., He, X., Bai, C., Wang, H., Wang, Q., Zuo, J., & Zheng, Y. 2024. "The regulatory mechanisms of delayed senescence of nitric oxide treatment of hyacinth beans." Postharvest Biology and Technology, 207, 112592. https://doi.org/10.1016/j.postharvbio.2023.112592

Higashiyama, T., & Yang, W. C. 2017. "Gametophytic pollen tube guidance: attractant peptides, gametic controls, and receptors". Plant Physiology, 173(1), 112–121. https://doi.org/10.1104/pp.16.01571

Kaya, H., Nakajima, R., Iwano, M., Kanaoka, M. M., Kimura, S., Takeda, S., Kawarazaki, T., et al. 2014. "Ca2+-activated reactive oxygen species production by Arabidopsis RbohH and RbohJ

is essential for proper pollen tube tip growth". The Plant Cell, 26(3), 1069–1080. https://doi.org/10.1105/tpc.113.120642

Khan, A. H., Wu, Y., Luo, L., Ma, Y., Li, Y., Ma, H., Luo, A., et al. 2022. "Proteomic analysis reveals that heat shock proteins enhance cotton male fertility under high-temperature stress by reducing ROS accumulation in anthers". Industrial Crops and Products, 188, 115693. https://doi.org/10.1016/j.indcrop.2022.115693

Kiani, R., Arzani, A., & Mir Mohammadi Mai body, S. A. M. 2021. "Polyphenols, flavonoids, and antioxidant activity involved in salt tolerance in wheat, Aegilops cylindrica and their amphidiploids". Frontiers in Plant Science, 12, 646221. https://doi.org/10.3389/fpls.2021.646221

Kim, D., Pertea, G., Trapnell, C., Pimentel, H., Kelley, R., & Salzberg, S. L. 2013. "TopHat2: accurate alignment of transcriptomes in the presence of insertions, deletions and gene fusions". Genome Biology, 14(4), R36. https://doi.org/10.1186/gb-2013-14-4-r36

Ku, T., Gu, H., Li, Z., Tian, B., Xie, Z., Shi, G., Chen, W., Wei, F., & Cao, G. 2022. "Developmental differences between anthers of diploid and autotetraploid rice at meiosis". Plants, 11(13), 1647. https://doi.org/10.3390/plants11131647

Langmead, B., & Salzberg, S. L. 2012. "Fast gapped-read alignment with Bowtie 2". Nature Methods, 9(4), 357–359.

Li Bao, C., Shiting, L., Chen, Z., & Shuyan, L. 2024. "NnARF17 and NnARF18 from lotus promote root formation and modulate stress tolerance in transgenic Arabidopsis thaliana". BMC Plant Biology, 24(1), 163. https://doi.org/10.1186/s12870-024-04852-9

Li, D., Sheng, Y., Niu, H., & Li, Z. 2019. "Gene interactions regulating sex determination in cucurbits". Frontiers in Plant Science, 10, 1231. https://doi.org/10.3389/fpls.2019.01231

Li, X., Shahid, M. Q., Xia, J., Lu, Z., Fang, N., Wang, L., Wu, J., Chen, Z., & Liu, X. 2017. "Analysis of small RNAs revealed differential expressions during pollen and embryo sac development in autotetraploid rice". BMC Genomics, 18(1), 129. https://doi.org/10.1186/s12864-017-3526-8

Liu, H., Li, J., Xu, C., Liu, H., & Zhao, Z. 2024. “Unravelling the molecular regulation network of carbon and lipid metabolism during seed development in Akebia trifoliata via integrated multi-omics analysis”. Scientific Reports, 14(1), 22893. https://doi.org/10.1038/s41598-024-74075-3

Livak, K. J., & Schmittgen, T. D. 2001. “Analysis of relative gene expression data using real-time quantitative PCR and the 2−ΔΔCT method”. Methods, 25, 402–408. https://doi.org/10.1006/meth.2001.1262

Lloyd, A., & Bomblies, K. 2016. “Meiosis in autopolyploid and allopolyploid Arabidopsis”. Current Opinion in Plant Biology, 30, 116–122. https://doi.org/10.1016/j.pbi.2016.02.004

Lu, L., Yang, W., Dong, Z., Tang, L., Liu, Y., Xie, S., & Yang, Y. 2023. “Integrated transcriptomic and metabolomics analyses reveal molecular responses to cold stress in coconut (Cocos nucifera L.) seedlings”. International Journal of Molecular Sciences, 24(19), 14563. https://doi.org/10.3390/ijms241914563

Luo, D., Ding, Q., Ma, X., Zhu, J., Zou, K., Hong, W., Wang, J., et al. 2023. “Proteomic and physiological responses of contrasting orchardgrass genotypes to heat stress”. International Journal of Biological Macromolecules, 245, 125463. https://doi.org/10.1016/j.ijbiomac.2023.125463

Martínez, C., & Jamilena, M. 2021. “To be a male or a female flower, a question of ethylene in cucurbits”. Current Opinion in Plant Biology, 59, 101981. https://doi.org/10.1016/j.pbi.2020.101981

Meyer, K., Cusumano, J. C., Somerville, C., & Chapple, C. 1996. “Ferulate-5-hydroxylase from Arabidopsis thaliana defines a new family of cytochrome P450-dependent monooxygenases”. Proceedings of the National Academy of Sciences, 93(14), 6869–6874. https://doi.org/10.1073/pnas.93.14.6869

Nabi, R. B. S., Tayade, R., Imran, Q. M., Hussain, A., Shahid, M., & Yun, B. W. 2020. “Functional insight of nitric-oxide induced DUF genes in Arabidopsis thaliana”. Frontiers in Plant Science, 11, 1041. https://doi.org/10.3389/fpls.2020.01041

Nawaz, M., Pan, J., Liu, H., Feng, K., Liu, J., Yang, W., Lv, Z., Zhang, Q., & Jiao, Z. 2026. “Multi-targeted antifungal mechanism of punicalagin against Botrytis cinerea and its role in preserving

strawberry quality". Postharvest Biology and Technology, 234, 114156. https://doi.org/10.1016/j.postharvbio.2026.114156

Ohnishi, T., Godza, B., Watanabe, B., Fujioka, S., Hategan, L., Ide, K., Shibata, K., Yokota, T., Szekeres, M., & Mizutani, M. 2012. "CYP90A1/CPD, a brassinosteroid biosynthetic cytochrome P450 of Arabidopsis, catalyzes C-3 oxidation". Journal of Biological Chemistry, 287(37), 31551–31560. https://doi.org/10.1074/jbc.M112.392720

Park, S. Y., Fung, P., Nishimura, N., Jensen, D. R., Zhao, Y., Lumba, S., et al. 2009. "Abscisic acid inhibits type 2C protein phosphatases via the PYR/PYL family of START proteins". Science, 324(5930), 1068–1071. https://doi.org/10.1126/science.1173041

Qadir, M., Wang, X., Shah, S. R. U., Zhou, X. R., Shi, J., & Wang, H. 2021. "Molecular network for regulation of ovule number in plants". International Journal of Molecular Sciences, 22(23), 12965. https://doi.org/10.3390/ijms222312965

Qi, W., Zhu, J., Wu, Q., Wang, Q., Li, X., Yao, D., Jin, Y., Wang, G., & Song, R. 2016. "Maize reas1 mutant stimulates ribosome use efficiency and triggers distinct transcriptional and translational responses". Plant Physiology, 170(2), 971–988. https://doi.org/10.1104/pp.15.01722

Ramsey, J., & Schemske, D. W. (2002). Neopolyploidy in flowering plants. *Annual Review of Ecology and Systematics*, *33*(1), 589–639. https://doi.org/10.1146/annurev.ecolsys.33.010802.150437

Ren, H., & Gray, W. M. 2015. "SAUR proteins as effectors of hormonal and environmental signals in plant growth". https://doi.org/10.1016/j.molp.2015.05.003

Riaz, M. W., Yousaf, M. I., Hussain, Q., Yasir, M., Sajjad, M., & Shah, L. 2023. "Role of lignin in wheat plant for the enhancement of resistance against lodging and biotic and abiotic stresses". Stresses, 3(2), 434–453. https://doi.org/10.3390/stresses3020032

Sankaranarayanan, S., Ju, Y., & Kessler, S. A. (2020). Reactive oxygen species as mediators of gametophyte development and double fertilization in flowering plants. Frontiers in Plant Science, 11, 1199. https://doi.org/10.3389/fpls.2020.01199

Sarkar, N. K., Kim, Y. K., & Grover, A. 2009. “Rice sHsp genes: genomic organization and expression profiling under stress and development”. BMC Genomics, 10(1), 393. http://www.biomedcentral.com/1471-2164/10/393

Sattler, M. C., Carvalho, C. R., & Clarindo, W. R. 2016. “The polyploidy and its key role in plant breeding”. Planta, 243, 281–296. DOI 10.1007/s00425-015-2450-x

Severyns, A., Claessen, H., Swennen, R., Janssens, S. B., Simba, R., Brown, A., & De Storme, N. 2025. “Functional analysis of pollen tube growth dynamics in banana (Musa spp.)”. Scientia Horticulturae, 349, 114268. https://doi.org/10.1016/j.scienta.2025.114268

Shi, F., Wang, Y., Huang, S., Dong, S., Liu, Z., & Feng, H. 2020. “Investigation of genes associated with petal variations between diploid and autotetraploid in Chinese cabbage (Brassica rapa L. ssp. pekinensis) by RNA-seq and sRNA-seq”. Molecular Genetics and Genomics, 295(6), 1459–1476. https://doi.org/10.1007/s00438-020-01713-6

Singh, R., Shankar, R., Yadav, S. K., & Kumar, V. 2023. “Transcriptome analysis of ovules offers early developmental clues after fertilization in Cicer arietinum L.” 3 Biotech, 13(6), 177. https://doi.org/10.1007/s13205-023-03599-8

Spartz, A. K., Ren, H., Park, M. Y., Grandt, K. N., Lee, S. H., Murphy, A. S., Sussman, M. R., Overvoorde, P. J., & Gray, W. M. 2014. “SAUR inhibition of PP2C-D phosphatases activates plasma membrane H+-ATPases to promote cell expansion in Arabidopsis”. The Plant Cell, 26(5), 2129–2142. https://doi.org/10.1105/tpc.114.126037

Staswick, P. E., Serban, B., Rowe, M., Tiryaki, I., Maldonado, M. T., Maldonado, M. C., & Suza, W. 2005. “Characterization of an Arabidopsis enzyme family that conjugates amino acids to indole-3-acetic acid”. The Plant Cell, 17(2), 616–627. https://doi.org/10.1105/tpc.104.026690

Stepanova, A. N., & Alonso, J. M. 2009. “Ethylene signaling and response: where different regulatory modules meet”. Current Opinion in Plant Biology, 12(5), 548–555. https://doi.org/10.1016/j.pbi.2009.07.009

Sudo, M., Yasuda, K., Yahata, M., Sato, M., Tominaga, A., Mukai, H., Ma, G., Kato, M., & Kunitake, H. 2021. “Morphological characteristics, fruit qualities and evaluation of reproductive

functions in autotetraploid Satsuma Mandarin (Citrus unshiu)". Agronomy, 11(12), 2441 https://www.mdpi.com/2073-4395/11/12/2441#.

Sugiyama, K. 2001. "Studies on breeding of watermelon for female flower-bearing ability and cracking resistance".

Sun, W., Van Montagu, M., & Verbruggen, N. 2002. "Small heat shock proteins and stress tolerance in plants". Biochimica et Biophysica Acta, 1577(1), 1–9. https://doi.org/10.1016/S0167-4781(02)00417-7

Tohge, T., Watanabe, M., Hoefgen, R., & Fernie, A. R. 2013. "The evolution of phenylpropanoid metabolism in the green lineage". Critical Reviews in Biochemistry and Molecular Biology, 48(2), 123–152. https://doi.org/10.3109/10409238.2012.758083

Tong, Y., Du, H., Xiao, J., Zhou, B., Zheng, X., Deng, Y., Zheng, X., & Chen, M. 2025. "Watermelon wilt disease: causes, harms, and control measures". Frontiers in Microbiology, 16, 1601130. https://doi.org/10.3389/fmicb.2025.1601130

Wang, C., Wang, T., Yin, M., Eller, F., Liu, L., Brix, H., & Guo, W. 2021. "Transcriptome analysis of tetraploid and octoploid common reed (Phragmites australis)". Frontiers in Plant Science, 12, 653183. https://doi.org/10.3389/fpls.2021.653183

Wang, S., Long, C., Liu, H., Pan, L., Yang, S., Zhao, J., Jiang, Y., & Bei, X. (2023). Comparative physiochemical and transcriptomic analysis reveals the influences of cross-pollination on ovary and fruit development in pummelo (Citrus maxima). Scientific Reports, 13, 19109. https://doi.org/10.1038/s41598-023-46058-3

Wang, Z. Y., Wang, Q., Chong, K., Wang, F., Wang, L., Bai, M., & Jia, C. 2006. "The brassinosteroid signal transduction pathway". Cell Research, 16(5), 427–434. https://doi.org/10.1038/sj.cr.7310054.

Wang, Z., Yadav, V., Yan, X., Cheng, D., Wei, C., & Zhang, X. 2021. "Systematic genome-wide analysis of the ethylene-responsive ACS gene family: Contributions to sex form differentiation and development in melon and watermelon". Gene, 805, 145910. https://doi.org/10.1016/j.gene.2021.145910

Westermann, J., Srikant, T., Gonzalo, A., Tan, H. S., & Bomblies, K. 2024. “Defective pollen tube tip growth induces neo-polyploid infertility”. https://doi.org/10.1126/science.adh0755

Wijesinghe, S. A. E. C., Evans, L. J., Kirkland, L., & Rader, R. 2020. “A global review of watermelon pollination biology and ecology: The increasing importance of seedless cultivars”. Scientia Horticulturae, 271, 109493. https://doi.org/10.1016/j.scienta.2020.109493

Yan, Z., Li, K., Li, Y., Wang, W., Leng, B., Yao, G., Zhang, F., Mu, C., & Liu, X. 2023. “The ZmbHLH32-ZmIAA9-ZmARF1 module regulates salt tolerance in maize”. International Journal of Biological Macromolecules, 253, 126978. https://doi.org/10.1016/j.ijbiomac.2023.126978

Yang, J. W., Park, S. U., Lee, H. U., Nam, K. J., Lee, K. L., Lee, J. J., Kim, J. H., Kwak, S. S., Kim, H. S., & Kim, Y. H. 2023. “Differential responses of antioxidant enzymes and lignin metabolism in susceptible and resistant sweet potato cultivars during root-knot nematode infection.” Antioxidants, 12(6), 1164. https://doi.org/10.3390/antiox12061164

Yang, Z., Chen, W., Jia, T., Shi, H., & Sun, D. 2023. “Integrated transcriptomic and metabolomic analyses identify critical genes and metabolites associated with seed vigor of common wheat”. International Journal of Molecular Sciences, 25(1), 526. https://doi.org/10.3390/ijms25010526

Yang, Z., Lin, M., Yang, X., Zhu, C., Wu, D., & Chen, K. 2023. “Mechanisms of the response of apple fruit to postharvest compression damage analyzed by integrated transcriptome and metabolome”. Food Chemistry: X, 20, 100972. https://doi.org/10.1016/j.fochx.2023.100972

Ye, C., Zheng, S., Jiang, D., Lu, J., Huang, Z., Liu, Z., Zhou, H., Zhuang, C., & Li, J. (2021). Initiation and execution of programmed cell death and regulation of reactive oxygen species in plants. International Journal of Molecular Sciences, 22(23), 12942. https://doi.org/10.3390/ijms222312942

Zeng, D., Que, C., Teixeira da Silva, J. A., Xu, S., & Li, D. 2022. “Comparative transcriptomic and metabolic analyses reveal the molecular mechanism of ovule development in the orchid, Cymbidium sinense”. Frontiers in Plant Science, 12, 814275. https://doi.org/10.3389/fpls.2021.814275

Zhang, Y. Z., Ma, Z. B., Li, W. H., Zhu, W., Gao, S. Q., Zhao, Y. H., & Liu, W. 2023. “Transcriptome and metabolome profiling reveals key pathways and metabolites involved in

defense against Verticillium dahliae in upland cotton." Industrial Crops and Products, 196, 116505. https://doi.org/10.1016/j.indcrop.2023.116505

Zhang, Y., Zhang, Y., Zhou, X., Yang, N., Zhou, D., Thakur, K., Wang, Q., et al. 2025. "Unraveling amino acid synthesis in mature sesame seeds based on integrative transcriptome and metabolome analysis." Food Frontiers, 6(2), 775–788. https://dx.doi.org/10.24272/j.issn.2095-8137.2024.266

Zhao, Y. 2012. "Auxin biosynthesis: a simple two-step pathway converts tryptophan to indole-3-acetic acid in plants". Molecular Plant, 5(2), 334–338.

Zhu, H., Zhao, S., Lu, X., He, N., Gao, L., Dou, J., Bie, Z., & Liu, W. 2018. "Genome duplication improves the resistance of watermelon root to salt stress". Plant Physiology and Biochemistry, 133, 11–21. https://doi.org/10.1016/j.plaphy.2018.10.019

Zu, S. H., Jiang, Y. T., Chang, J. H., Zhang, Y. J., Xue, H. W., & Lin, W. H. 2022. "Interaction of brassinosteroid and cytokinin promotes ovule initiation and increases seed number per silique in Arabidopsis". Journal of Integrative Plant Biology, 64(3), 702–716. https://doi.org/10.1111/jipb.13197

Zumajo-Cardona, C., & Ambrose, B. A. 2020. "Phylogenetic analyses of key developmental genes provide insight into the complex evolution of seeds". Molecular Phylogenetics and Evolution, 147, 106778. https://doi.org/10.1016/j.ympev.2020.106778

Supplementary Files

This is a list of supplementary files associated with this preprint. Click to download.

- S1.xlsx
- S2.xlsx
- S3.xls.xlsx
- S4.xlsx
- S5.xlsx